THE JOURNAL OF BIOLOGICAL CHEMISTRY VOL. 289, NO. 2, pp. 1033–1048, January 10, 2014

The Active Form of E6-associated protein (E6AP)/UBE3A Ubiquitin Ligase Is an Oligomer*[S]

Received for publication, September 10, 2013, and in revised form, November 22, 2013 Published, JBC Papers in Press, November 22, 2013, DOI 10.1074/jbc.M113.517805

Virginia P. Ronchi[‡], Jennifer M. Klein[‡], Daniel J. Edwards[‡], and Arthur L. Haas[‡§1]

From the [‡]Department of Biochemistry and Molecular Biology and the [§]Stanley S. Scott Cancer Center, Louisiana State University Health Sciences Center, New Orleans, Louisiana 70112

Background: E6AP/UBE3A is a Hect ligase implicated in neurodevelopment and cell transformation.
Results: Kinetic/biophysical analyses demonstrate that E6AP oligomerization is required for polyubiquitin degradation signal assembly and that changes in oligomerization regulates such activity.
Conclusion: E6AP oligomerization accounts for opposing effects of mutation and HPV16/18 E6 protein.
Significance: These findings explain in part the etiology of specific Angelman syndrome mutations and E6-mediated cell transformation.

Employing ^{125}I-polyubiquitin chain formation as a functional readout of ligase activity, biochemical and biophysical evidence demonstrates that catalytically active E6-associated protein (E6AP)/UBE3A is an oligomer. Based on an extant structure previously discounted as an artifact of crystal packing forces, we propose that the fully active form of E6AP is a trimer, analysis of which reveals a buried surface of 7508 Å^2 and radially symmetric interacting residues that are conserved within the Hect (homologous to E6AP C terminus) ligase superfamily. An absolutely conserved interaction between Phe^{727} and a hydrophobic pocket present on the adjacent subunit is critical for trimer stabilization because mutation disrupts the oligomer and decreases k_{cat} 62-fold but fails to affect E2∼ubiquitin binding or subsequent formation of the Hect domain Cys^{820}∼ubiquitin thioester catalytic intermediate. Exogenous *N*-acetylphenylalanylamide reversibly antagonizes Phe^{727}-dependent trimer formation and catalytic activity (K_i = 12 mM), as does a conserved α-helical peptide corresponding to residues 474–490 of E6AP isoform 1 (K_i = 22 μM) reported to bind the hydrophobic pocket of other Hect ligases, presumably blocking Phe^{727} intercalation and trimer formation. Conversely, oncogenic human papillomavirus-16/18 E6 protein significantly enhances E6AP catalytic activity by promoting trimer formation ($K_{activation}$ = 1.5 nM) through the ability of E6 to form homodimers. Recombinant E6 protein additionally rescues the k_{cat} defect of the Phe^{727} mutation and that of a specific loss-of-function Angelman syndrome mutation that promotes trimer destabilization. The present findings codify otherwise disparate observations regarding the mechanism of E6AP and related Hect ligases in addition to suggesting therapeutic approaches for modulating ligase activity.

E6AP[2]/UBE3A is the founding member of the Hect (homologous to E6AP C terminus) ubiquitin ligase family and is defined by a highly conserved 350-residue C-terminal catalytic domain (1, 2). The Hect domain is characterized by the presence of an active site cysteine that forms an obligatory high energy thioester bond with ubiquitin prior to transfer of the latter to specific substrate proteins, the identity of which is defined by the N-terminal targeting domain (2). The E6AP Hect domain assembles Lys^{48}-linked polyubiquitin degradation signals that are recognized by the 26 S proteasome (3, 4). Both activation and loss of E6AP function are implicated in various human diseases, as discussed elsewhere (5–7). Abrogation of E6AP function by deletion, imprinting defects, or mutation of the *UBE3A* gene locus within the 15q11–13 chromosome region is associated with the neurological disorder Angelman syndrome (8–10). Patients affected with Angelman syndrome are characterized by severe intellectual and developmental disability, speech impairment, behavioral uniqueness, epilepsy, and severely abnormal electroencephalography, among other symptoms (11–14). Most of the naturally occurring mutations within the *UBE3A* gene introduce deletions that generate truncated forms of E6AP lacking the intact Hect domain; however, ∼10% of the genetic alterations correspond to point mutations within the E6AP coding region (15, 16). Although many of the point mutants represent loss-of-function alterations and are not able to ubiquitinate their substrate, paradoxically, many retain the ability to form a thioester bond with ubiquitin (17). In contrast, duplication of the corresponding *UBE3A* gene is thought to result in some cases of autism spectrum disorder (18–21). These observations suggest a narrow range of E6AP activity for normal neurological development because *UBE3A*-deficient mouse models or those expressing higher levels of the

* This work was supported, in whole or in part, by National Institutes of Health Grant GM034009 (to A. L. H.).
[S] This article contains supplemental Tables 1 and 2 and Fig. 1.
[1] To whom correspondence should be addressed: Dept. of Biochemistry and Molecular Biology, LSU Health Sciences Center, 1901 Perdido St., New Orleans, LA 70112. Tel.: 504-568-3004; Fax: 504-568-2093; E-mail: ahaas@lsuhsc.edu.

[2] The abbreviations used are: E6AP, E6-associated protein (gene name *UBE3A*); E6, human papilloma virus 16 E6 protein; Hect, homologous to E6AP C terminus; HPV, human papilloma virus; Ac-PheNH$_2$, *N*-acetylphenylalanylamide; E1, generic term for activating enzymes of Class 1 ubiquitin-like proteins; E2/Ubc, generic name for ubiquitin carrier protein/ubiquitin-conjugating enzyme; E3, generic name for ubiquitin:protein isopeptide ligase; UbcH7, human E2 carrier protein (gene name *UBE2L3*); Uba1, ubiquitin-activating enzyme (gene name *UBE1*).

ligase show phenotypes similar to Angelman syndrome or autism, respectively (18, 22–24). In general, the clinical symptoms associated with the neurological disorders and the identified targets of E6AP-catalyzed ubiquitination localize to regulatory pathways required for synaptic plasticity (25–29). The identification of Arc and Ephexin 5 as targets of E6AP, both of which function to mediate synaptic remodeling, provide a framework for reconciling the loss-of-function mutations in the E6AP maternal copy and the neurological and developmental defects present in affected individuals (25, 26, 30), although more recent evidence questions a role for E6AP in targeting Arc degradation (30).

The E6AP protein was initially identified by its interaction with the E6 viral protein encoded by human papilloma virus 16 (HPV16) (31–33). Although p53 degradation is normally mediated by the Mdm2 ubiquitin ligase (34), E6 protein is proposed to bind to E6AP and redirect its specificity to p53 (33, 35). Enhanced degradation of p53 in epithelial cells by the HPV16 and -18 viral strains induces cell transformation and development of cervical and oral cancers, depending on the site of infection (5, 36, 37). Similarly, hepatitis C virus encodes the NS5B protein that binds E6AP and induces degradation of the retinoblastoma protein tumor suppressor, increasing the risk of liver cirrhosis and hepatocellular carcinoma (38, 39). The E6AP sequence contains a leucine-rich motif (L*XX*LL) in the N-terminal region to which the E6 viral protein binds (40–42). Biophysical and structural analyses of the E6-E6AP interaction show that the N-terminal E6 Zn^{2+}-binding domain primarily interacts with E6AP, whereas the C-terminal Zn^{2+}-binding domain interacts with p53 (43–47). Although the interaction of E6 with E6AP is necessary for degradation of p53, the effect of such interaction on the catalytic activity of E6AP has not been adequately addressed; Kao *et al.* (48) have shown that ectopic E6 expression increases E6AP autoubiquitination and intracellular turnover.

Full-length E6AP is a protein of 100 kDa; however, only the structure of the truncated E6AP Hect domain in association with its cognate UbcH7 ubiquitin carrier protein has been reported (49). The Hect domain architecture displays an L-shape with distinct N-terminal and C-terminal subdomains connected by a flexible hinge region (49). The N-terminal subdomain can be further divided into large and small N-terminal subdomains also connected by flexible hinge segments (49). The active site Cys^{820} to which ubiquitin forms a thioester intermediate is contained in the C-terminal subdomain (49, 50). The UbcH7 carrier protein binds to a pocket in the small N-terminal subdomain, but the geometry of the bound UbcH7~ubiquitin thioester relative to Cys^{820} has been a challenge to understanding within the context of a coherent mechanism for Cys^{820}~ubiquitin thioester formation and subsequent polyubiquitin chain formation, discussed recently (51). However, we have used kinetic analysis of ^{125}I-polyubiquitin chain assembly to demonstrate for the first time the presence of two functionally distinct E2~ubiquitin binding sites on the E6AP Hect domain, providing a mechanistically tractable resolution to the problem of active site thioester formation (51). Other kinetic evidence indicates that the canonical UbcH7 binding site presented in the original crystal structure (49) functions in chain elongation from the ubiquitin thioester formed at Cys^{820} (51), providing an entre into reconciling a potential mechanism for polyubiquitin chain assembly.

In the present work, we use kinetic and biophysical methods to demonstrate for the first time that an E6AP oligomer is the catalytically competent form of the enzyme. Based on an earlier structure for E6AP initially discounted as an artifact of crystal packing forces (49), we propose that the fully functional form of the oligomer is a trimer, computational analysis of which allowed us to identify conserved residues located at the subunit interfaces. Using rates of ^{125}I-polyubiquitin chain assembly as a functional readout, we have identified a subset of residues essential for stabilizing the active trimer. Furthermore, a small molecule mimic of a key stabilizing interaction is sufficient to dissociate the trimer and abrogate E6AP-catalyzed chain assembly but not Cys^{820}~ubiquitin thioester formation. In contrast, E6 viral protein enhances E6AP activity by promoting oligomerization as a consequence of the ability of the former to dimerize through its N-terminal Zn^{2+} binding domain (51, 52). Remarkably, E6-induced oligomerization rescues synthetic and Angelman syndrome loss-of-function mutations contributing to subunit association and stabilization. The current results explain previously unresolved roles for a cohort of point mutations in the neurological pathology of Angelman syndrome, reveal new strategies for regulating E6AP function by modulating subunit assembly, and provide insights into the role of oligomerization in polyubiquitin chain formation by the Hect ligase superfamily.

MATERIALS AND METHODS

Bovine ubiquitin and creatine phosphokinase were purchased from Sigma. Ubiquitin was further purified to apparent homogeneity by FPLC and quantitated spectrophotometrically (53). Ubiquitin was radioiodinated by the Chloramine-T procedure to yield a specific radioactivity of ~15,000 cpm/pmol using carrier-free Na^{125}I purchased from either GE Healthcare or PerkinElmer Life Sciences (54). Human erythrocyte Uba1 (UBA1) was purified to apparent homogeneity from outdated human blood (54). Active Uba1 was quantitated by the stoichiometric formation of ^{125}I-ubiquitin thioester (54–56). Human recombinant UbcH7 (UBE2L3) was that described previously (57, 58), and active E2 concentration was quantitated by the Uba1-dependent stoichiometric formation of UbcH7~^{125}I-ubiquitin thioester (51, 59). The E2 protein was stored at −80 °C in small aliquots and was stable for more than 6 months although subject to activity loss with successive freeze-thaw cycles (59). The *N*-acetyl-L-phenylalanylamide (Ac-PheNH_2; E-1160) was obtained from Bachem Americas. The *N*-acetyl-NRIRMYSERRITVLYSL peptide (purity >95%) was obtained from PEPTIDE 2.0 Inc.

Generation and Purification of Recombinant E6AP—Human E6AP isoform 3 (*UBE3A*; IMAGE clone NM00046.2) was subcloned into pGEX4T1 to yield pGEX4T1-E6AP as described previously (51).[3] The E6APF727D, E6APY533A, E6APD543A,

[3] The sequence for E6AP isoform 3 differs from isoform 1, from which the original crystal structure was determined (49), by the presence of an additional 20 amino acids at the N terminus. To facilitate comparison with the crystal structure, residues for isoform 3 will be referenced to the paralogous position of isoform 1 (*i.e.* by subtracting 20 from the isoform 3 residue number).

E6APR626A, and E6APK688A mutants were generated from pGEX4T1-E6AP using the QuikChange protocol of Stratagene to yield pGEX4T1-E6APF727D, pGEX4T1-E6APY533A, pGEX4T1-E6APD543A, pGEX4T1-E6APR626A, and pGEX4T1-E6APK688A, respectively. The E6APΔ495 truncation lacking the C-terminal Hect domain was generated by inserting a STOP codon after codon 495 of pGEX4T1-E6AP to yield pGEX4T1-E6APΔ495. Residues 450–852 of full-length E6AP were subcloned by PCR into the BamHI/NotI sites of pGEX4T1 to yield pGEX4T1-E6AP-Hect, from which was expressed the GST-E6AP-Hect domain fusion protein. The active site Cys^{820} was similarly mutated to alanine by the QuikChange protocol to yield GST-E6AP-HectC820A protein. The coding regions for all E6AP clones were sequenced to preclude cloning artifacts and to verify the desired mutation. Wild type and mutant GST-E6AP proteins were expressed and purified as described previously (51, 58). The activities of GST-E6AP and its mutants were quantitated by their stoichiometric formation of ^{125}I-ubiquitin thioester (51, 59, 60). Unless otherwise noted, the GST moiety was not processed from the fusion proteins by thrombin digestion (51).

The full-length E6AP sequence was subsequently cloned by PCR into the BamHI/HindIII sites of pFastBac Htb (Invitrogen) for baculoviral expression of the corresponding His_6-E6AP. After bacmid amplification, the complete insert was sequenced to confirm the absence of cloning errors. The bacmid was transfected into Sf9 insect cells, and then the P1 virus was isolated and amplified as a P2 stock. The P2 stock was then used to transfect Sf9 cells (3.6×10^7 cells/T45 flask, 10^5 virus particles/T45flask), and protein expression was allowed to proceed for 5 days as recommended by the Bac-to-Bac Baculovirus Expression System manual (Invitrogen). Full-length recombinant His_6-E6AP was isolated from the medium by affinity purification using a 1.5 × 3.0-cm HisTrap HP column (Amersham Biosciences). The column was equilibrated in 50 mM Tris-HCl (pH 8.0) and 20 mM imidazole, and the bound protein was eluted in 50 mM Tris-HCl (pH 8.0) containing 300 mM imidazole. After elution, the protein was equilibrated by dialysis into 50 mM Tris-HCl (pH 7.5) containing 300 mM NaCl and 1 mM DTT. Typically 1.6–2 mg of affinity-purified His_6-E6AP protein could be isolated from 13 T150 flasks, of which 10–40% was active by the Uba1-dependent formation of E6AP~^{125}I-ubiquitin thioester (51, 58).

Expression and Purification of Recombinant HPV16 E6 Protein—HPV16 E6 protein coding sequence (GenBank™ EF122273.1; GI 119710759) was subcloned into BamHI/XhoI sites of pGEX4T3 to yield pGEX4T3-E6(HPV16). The E6(HPV16)Δ91 recombinant protein was obtained by inserting a STOP codon after codon 91 by the QuikChange protocol of Stratagene to yield pGEX4T3-E6(HPV16)Δ91. The HPV16 E6 C-terminal domain corresponded to residues 89–158 and was subcloned into BamHI/XhoI sites of pGEXT4T1 by PCR to yield pGEX4T1-E6Ct. *Escherichia coli* BL21 (DE3) cells harboring pGEX-E6(HPV16), pGEX4T3-E6(HPV16)Δ91, or pGEX4T1-E6(HPV16)E6Ct were grown at 37 °C and then induced at A_{600} of 0.6 by the addition of isopropyl-1-thio-β-D-galactopyranoside to a final concentration of 0.4 mM. After 3 h at 37 °C, cells were harvested by centrifugation at 6000 × *g* for 30 min and then resuspended in 50 mM Tris-HCl (pH 7.5) containing 150 mM NaCl and 1 mM DTT (59). Cells were lysed by Emulsiflex (Avestin) and then centrifuged at 30,000 × *g* for 30 min (59). Recombinant GST-E6(HPV16) fusion proteins were purified on glutathione-Sepharose, processed with thrombin, and then passed through a second glutathione-Sepharose column to remove free GST (59). The total protein content calculated by the theoretical 280 nm extinction coefficient yielded 2.4 mg/liter of culture except for E6(HPV16)Δ91, which yielded 0.5 mg/liter of culture. The proteins were flash frozen in small aliquots and stored at −80 °C.

E6AP-catalyzed ^{125}I-Ubiquitin Conjugation Assay—The E3 ligase activity of recombinant E6AP was quantitated in kinetic assays under initial velocity conditions (51, 58). Rates of E6AP-catalyzed ^{125}I-polyubiquitin chain formation were measured at 37 °C in incubations of 25-μl final volume containing 50 mM Tris-HCl (pH 7.5), 1 mM ATP, 10 mM $MgCl_2$, 1 mM DTT, 10 mM creatine phosphate, 1 IU of creatine phosphokinase, 5 μM ^{125}I-ubiquitin (~1.5×10^4 cpm/pmol), 50 nM human Uba1, and the indicated concentrations of UbcH7 and E6AP (59, 61). Reactions were initiated by the addition of ^{125}I-ubiquitin. After 10–30 min, the reactions were quenched by the addition of 25 μl of 2× SDS sample buffer containing 0.3% (v/v) β-mercaptoethanol, and then the samples were heated to 100 °C for 3 min. The polyubiquitin conjugates were resolved from free ^{125}I-ubiquitin by 12% (w/v) SDS-PAGE under reducing conditions at 4 °C and visualized by autoradiography of the dried gels (59, 61). Polyubiquitin chain formation was measured by excising lanes between the top of the resolving gel and the top of the stacker gel, representing anchored and free ^{125}I-polyubiquitin chains, respectively (62), and quantitating associated ^{125}I-ubiquitin by γ-counting (51, 59, 61). Absolute rates of ^{125}I-polyubiquitin chain formation were calculated from the associated radioactivity and the corrected specific radioactivity for ^{125}I-ubiquitin (51, 59, 61). Datum points represent single assay determinations, and complete data sets were evaluated by nonlinear regression analysis using GraFit version 5.0 (Erithicus). Active Uba1, E2, and E6AP were independently determined in parallel by their stoichiometric formation of ^{125}I-ubiquitin thioester (59).

Static Light-scattering Measurements—His_6-E6AP after the His trap affinity purification step was further purified by FPLC using a Mono Q 5/50 column (Amersham Biosciences) equilibrated in 50 mM Tris-HCl (pH 7.5) and 1 mM DTT. Recombinant His_6-E6AP eluted at 300 mM NaCl in a 0–500 mM gradient (16 mM/ml, 1 ml/min). The molecular weight of His_6-E6AP was determined in solution at 37 °C by static light scattering using a 235-DynaPro NanoStar laser light scattering spectrometer at 663 nm wavelength (Wyatt Technology Corp.). Spectra were collected for 18 μM His_6-E6AP in 50 mM Tris-HCl (pH 7.5) containing 200 mM NaCl. The effect of Ac-PheNH_2 on the molecular weight of His_6-E6AP was determined in 50 mM Tris-HCl (pH 7.5) containing 200 mM NaCl, 16 μM His_6-E6AP total protein, 61 mM Ac-PheNH_2, and 8% (v/v) carrier methanol. The molecular weight of E6AP was also evaluated in reactions containing 0–350 μM Ac-NRIRMYSERRITVLYSL in 50 mM Tris-HCl (pH 7.5), 250 mM NaCl, 1 mM DTT, and 17 μM His_6-E6AP. Data were analyzed with Dynamics® software at both default

and maximum sensitivity to detect the presence of low concentrations of E6AP oligomeric forms.

Analysis of E6AP-Hect Interface Structure—The E6AP Hect domain structure (PDB code 1D5F) corresponding to the E6AP trimer reported by Huang *et al.* (49) was analyzed using PISA (PDBePISA-EMBL-EBI (Protein Interfaces, Surfaces, and Assemblies)) (63). The Assemblies analysis predicted a strong interaction between subunits, and default conditions detected an average of 38 residues/subunit involved in surface interactions between adjacent subunits (63). All structural representations were generated with PyMOL (Schrödinger, LLC).

RESULTS

E6AP-catalyzed Polyubiquitin Chain Formation Requires Oligomerization—Early in our studies, we examined the effect of the GST moiety on E6AP activity and found that processing of GST-E6AP fusion protein with thrombin resulted in a consistent 15–30% decrease in activity that resulted from a proportionately lower k_{cat} but without effect on the K_m for UbcH7~^{125}I-ubiquitin binding (not shown). Because GST protein is known to dimerize (64–66), one interpretation posits that GST promotes oligomerization of E6AP that results in the increased k_{cat}. Consistent with this model, the addition of free GST to disrupt the putative oligomerization of GST-E6AP showed a biphasic concentration dependence (Fig. 1*A*). At free GST concentrations less than 5 μM, the abrupt concentration-dependent decrease in the initial rate of polyubiquitin chain formation exhibited a $K_{½}$ of ~1 μM, whereas at higher concentrations, there was a linear reduction in the initial rate with $[GST]_o$ (Fig. 1*A*). The linear phase at higher GST concentrations coincided with the appearance of a band of monoubiquitinated GST and probably results from competition of this reaction with polyubiquitin chain elongation. In contrast, the decrease in rate occurring at lower GST concentrations was consistent with disruption of GST-E6AP homodimers by free GST because the K_d for GST dimerization is 0.6 μM (66).

To directly evaluate the potential contribution of E6AP oligomerization to catalytic activity, we introduced a STOP codon in the GST-E6AP coding region to truncate the Hect domain from E6AP, generating GST-E6APΔ495, to test whether the truncated protein could disrupt oligomerization in a manner similar to the free GST moiety. The addition of either 54 μM GST-E6APΔ495 or 66 μM thrombin-processed E6APΔ495 to wild type enzyme decreased the initial rate of GST-E6AP-catalyzed polyubiquitin chain formation (Fig. 1*B*). When the experiment of Fig. 1*B* was repeated at different concentrations of either GST-E6APΔ495 or E6APΔ495, hyperbolic concentration-dependent decreases in the initial rates of polyubiquitin chain formation resulted (Fig. 1, *C* and *D*, respectively). At higher concentrations than shown in Fig. 1, *C* and *D*, GST-E6APΔ495 and E6APΔ495 quantitatively blocked wild type GST-E6AP-catalyzed polyubiquitin chain formation (not shown). Nonlinear hyperbolic regression analysis yielded K_i values of 12 ± 3 and 19 ± 8 μM for GST-E6APΔ495 and E6APΔ495, corresponding to $\Delta G_{binding}$ values of −6.7 and −6.4 kcal/mol, respectively. Although the individual K_i values are not statistically different, the corresponding $\Delta\Delta G_{binding}$ for contribution of the GST moiety to GST-E6AP dimerization predicts a K_d for GST association of 1.6 μM, in good agreement with the published value of 0.6 μM (66). Results identical to those of Fig. 1, *C* and *D*, were obtained when the experiments were repeated with catalytically inactive GST-E6AP-HectC820A or E6AP-HectC820A in which the active site Cys^{820} of the Hect domain was mutated to alanine, yielding K_i values of 31 ± 4 and 27 ± 9 μM, respectively (Fig. 1*E*). Inhibition by E6APΔ495 is consistent with a model in which the truncation competitively disrupts an intrinsic E6AP wild type oligomer that is required for activity, schematically illustrated in Fig. 1*F*. Overall, the data reveal that oligomerization of E6AP is required for catalytic competence in polyubiquitin chain assembly. The similarities in K_i values between the E6APΔ495 and E6AP-HectC820A proteins suggest that the Hect domain and the targeting regions both contribute to oligomerization.

Active E6AP Is an Oligomer—Resolution of bacterially expressed protein by SDS-PAGE and visualization by Coomassie staining revealed a series of GST-associated bands in our preparations ranging from a relative mobility of ~130 kDa for full-length protein, in good agreement with the expected size of 125 kDa, to 25 kDa, representing the free GST moiety (Fig. 2*A*, *left lane*); however, only the band of highest relative molecular weight, corresponding to full-length GST-E6AP, formed a ^{125}I-ubiquitin thioester (51). Because bacterially expressed recombinant GST-E6AP is isolated as a mixture of full-length and C-terminal truncations (Fig. 2*A*, *left*), the results of Fig. 1 suggest that our kinetic studies probably underestimate the intrinsic k_{cat} for the ligase due to the presence of endogenous GST-E6AP fragments. To test this, we cloned full-length E6AP into a baculovirus expression system to yield >95% full-length ligase. The resulting N-terminal His_6-E6AP could be isolated from the medium without the marked fragmentation observed for bacterially expressed GST-E6AP and exhibited a relative molecular mass of 100 kDa, corresponding to the predicted value for full-length protein (Fig. 2*A*, *right*). After purification, maintaining the protein in a low concentration of NaCl was essential to prevent protein precipitation upon removal of imidazole. On a lower percentage SDS-polyacrylamide gel, the full-length affinity-purified band could be resolved into two closely migrating bands, only the slower migrating band of which could be detected on Western blots using anti-His_6 antibody compared with detection by anti-E6AP antibody (Fig. 2*B*). A trace fragment band lacking the His_6 tag could also be detected by anti-E6AP Western blot (Fig. 2*B*). Co-purification of E6AP lacking the affinity tag with His_6-E6AP is consistent with oligomerization of the enzyme indicated by the results of Fig. 1.

We have previously demonstrated that the recombinant GST-E6AP in preparations identical to that analyzed in Fig. 2*A* (*left*) exhibited hyperbolic kinetics for ^{125}I-polyubiquitin chain formation with respect to $[UbcH7]_o$, from which values of K_m and k_{cat}, the latter defined as $V_{max}/[GST\text{-}E6AP]_o$, could be determined (51). Baculovirally expressed His_6-E6AP also yielded hyperbolic kinetics for ^{125}I-polyubiquitin chain formation with respect to $[UbcH7]_o$ from which K_m (46 ± 7 nM) and k_{cat} (0.63 ± 0.03 s^{-1}) could be determined by nonlinear hyperbolic regression analysis (51) (Table 1). That homogeneous full-length E6AP exhibits a K_m indistinguishable from that of the bacterially expressed heterogeneous GST-E6AP preparations,

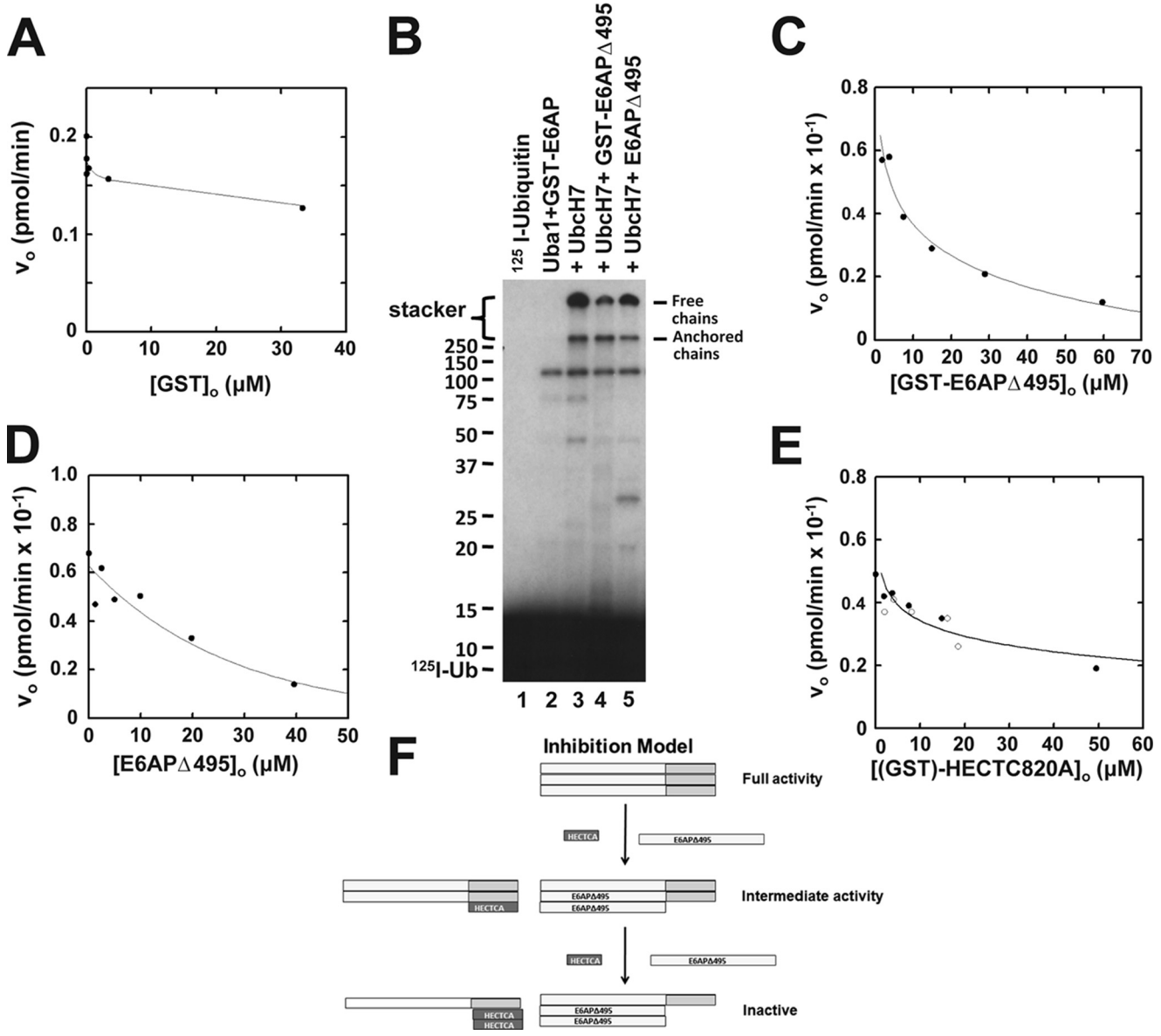

FIGURE 1. **E6AP catalyzed polyubiquitin chain formation requires oligomerization.** *A*, initial rates of E6AP-catalyzed free polyubiquitin chain formation were determined as described under "Materials and Methods" in the presence of 8 nM human Uba1, 200 nM UbcH7, 0.2 nM GST-E6AP, 5 μM ^{125}I-ubiquitin, and the indicated concentrations of recombinant free GST. *B*, autoradiogram of ^{125}I-ubiquitin conjugation assays performed under initial velocity conditions in the presence of 60 nM human Uba1, 400 nM UbcH7, 6 nM GST-E6AP, 4 μM ^{125}I-ubiquitin, and either 54 μM GST-E6APΔ495 or 66 μM E6APΔ495, as indicated. *C*, initial rates of ^{125}I-ubiquitin conjugation were determined as in *B* in the presence of 8 nM GST-E6AP and the indicated concentrations of GST-E6APΔ495. As described under "Materials and Methods," radioactivity associated with the stacker gel representing free and unanchored ^{125}I-polyubiquitin chains was quantitated to calculate the resulting initial velocities. *D*, initial rates of ^{125}I-ubiquitin conjugation were determined as in *C* but with the indicated concentrations of E6APΔ495. *E*, initial rate assays of ^{125}I-ubiquitin conjugation determined as in *C* in the presence of the indicated concentrations of GST-HectC820A (*open circles*) or HectC820A (*closed circles*). *F*, schematic diagram depicting the model for inhibition of polyubiquitin chain formation by the Δ495 truncation or free Hect domain. For *C–E*, *solid lines* represent nonlinear inverse hyperbolic regression fits of the data using GraFit version 5.0.

but a 20-fold higher k_{cat} is consistent with our prediction based on a model for oligomerization. Similarly, GST-E6AP Hect domain protein composed of residues 450–872 is capable of modest polyubiquitin chain formation and has an affinity for UbcH7~ubiquitin thioester ($K_m = 89 \pm 11$ nM) that is slightly less than that of full-length E6AP but a k_{cat} that is 2000-fold lower (Table 1). In contrast, removing the GST moiety by *in situ* processing with thrombin prior to assay abrogates chain formation (not shown); however, the resulting Hect domain moiety catalyzes a slow rate of monoubiquitination, as noted previously (51). The kinetics of Hect domain monoubiquitination follows hyperbolic kinetics with respect to [UbcH7]$_o$ and yields K_m and k_{cat} values similar to those of the unprocessed GST-Hect domain (Table 1). The results of Table 1 are not a consequence of differences in the amounts of active protein in the various preparations because in each case the ligase is quantitated by the functional assay of stoichiometric Hect domain~^{125}I-ubiquitin thioester formation. Therefore, polyubiquitin chain formation kinetics for the various forms of E6AP (Table 1) and the effect of N-terminal truncation (Fig. 1) are consistent with the catalytically active form of the enzyme existing as an oligomer.

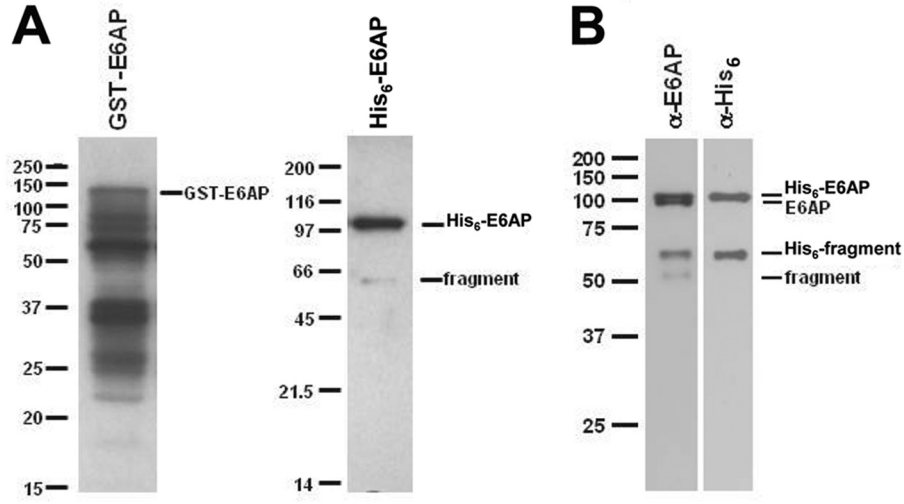

FIGURE 2. **SDS-PAGE of selected E6AP preparations.** *A*, Coomassie-stained 10% (w/v) SDS-PAGE resolution of affinity-purified recombinant GST-E6AP expressed in *E. coli* (*left*) *versus* His_6-E6AP expressed in baculovirus (*right*). *B*, Western blot of 12% (w/v) SDS-PAGE resolution of baculovirus-expressed His_6-E6AP stained with anti-E6AP antibody (*left*) and then stripped and restrained with anti-His_6 antibody (*right*). Mobility markers are shown to the *left* of the corresponding panels. Mobilities of selected E6AP species are shown to the *right* of the corresponding *panels*.

TABLE 1
Effect of E6AP length on chain formation kinetics

	K_m	k_{cat}	k_{cat}/K_m
	nM	s^{-1}	$M^{-1}\,s^{-1}$
Heterogeneous GST-E6AP	58 ± 6	$3.1 \pm 0.9 \times 10^{-2}$	5.4×10^5
E6AP Hect domain[a]	91 ± 25	$7.0 \pm 0.1 \times 10^{-4}$	8.5×10^3
GST-E6AP Hect domain	89 ± 11	$3.2 \pm 0.1 \times 10^{-4}$	3.6×10^3
Homogeneous His_6-E6AP	46 ± 7	$6.3 \pm 0.3 \times 10^{-1}$	1.3×10^7

[a] Determined by E6AP Hect domain monoubiquitination.

A Trimer Is the Likely Fully Active Form of E6AP—To test directly the ability of E6AP to oligomerize, we determined the solution molecular weight of wild type His_6-E6AP by gel filtration chromatography (Fig. 3*A*). The relative molecular weight for E6AP, monitored by ^{125}I-polyubiquitin chain formation under E3-limiting conditions, encompasses a peak centered at 190 kDa. This molecular weight is consistent with a stable dimer of 100-kDa subunits or less stable higher oligomers subject to dissociation by dilution as the complex passes through the column. To distinguish between the latter, we analyzed a parallel sample by static light scattering, which does not involve sample dilution. Following Mono Q anion exchange chromatography to remove inactive high molecular weight aggregates, freshly prepared active His_6-E6AP displayed a molecular mass of 283 kDa by static light scattering that was consistent with a trimer (Fig. 3*A*). The low abundance higher molecular weight species of ~50-nm radius represents aggregates not completely removed by the Mono Q FPLC step. In parallel experiments, the molecular mass ranged from ~200 to 400 kDa depending on protein concentration, pH, and ionic strength, consistent with equilibrium oligomerization of the 100-kDa monomer (not shown).

Wild type E6AP is thought to exist as a monomer; however, the original publication reporting the structure of the isolated Hect domain also noted a trimeric structure that was proposed to arise from crystal packing interactions (49) (Fig. 4*A*). Based on the data of Fig. 3 and the requirement that E6AP-catalyzed polyubiquitin chain formation requires oligomerization, we propose that the fully active form of the ligase is a trimer. The symmetric trimer (PDB code 1D5F) reported by Huang *et al.* (49) buries an extensive combined surface area of 7508 Å^2 comprising a large fraction of apolar residues at the subunit interfaces that represents a solvation free energy of −4.2 kcal/mol by PISA analysis (63) (Fig. 4*A*), corresponding to an apparent K_d of 25 μM for E6AP Hect subunit interactions without considering additional hydrogen bond or salt bridge interactions (supplemental Table 1), which are difficult mathematically to model due to uncertainties related to the actual microenvironments of the individual bonds. However, the predicted K_d based on desolvation agrees well with the empirical K_i obtained with GST-HectC820A (31 ± 4 μM) and HectC820A (27 ± 9 μM) (Fig. 1*D*). Sequence comparison among known Hect domain sequences reveals marked conservation (37% identity, 69% conservation of side chain polarity) among the residues at the subunit interfaces of the E6AP trimer (supplemental Fig. 1 and Table 2). Collectively, these features are characteristic of protein-protein binding interfaces rather than crystal packing interactions (67, 68). Moreover, the separation distance between N-terminal residues of the Hect domain subunits suggests that the N-terminal targeting domains of the subunits present on the full-length molecule would not hinder trimer formation (Fig. 4*B*).

As a trimer, the 1DF5 structure reveals a number of radially symmetric subunit interactions. For example, the large N-terminal subdomain of the Hect domain contains a subset of conserved apolar residues at the subunit interface (Ile^{600}, Tyr^{601}, Leu^{723}, Leu^{726}, Ile^{732}, and Leu^{735}) that forms a hydrophobic pocket into which intercalates Phe^{727} of the adjacent subunit in the trimer (49) (Fig. 4*C*), providing a stabilization of −2.13 kcal/mol by PISA analysis. Although there are other residues and surfaces contributing to stabilization of the trimer, intercalation of Phe^{727} into the hydrophobic pocket appears to be of special importance because mutation of Phe^{727} to alanine destabilizes trimeric E6AP in favor of the monomer, the latter of which retains the ability to form a ubiquitin thioester intermediate (49). Retention of the ability to form the thioester intermediate was originally interpreted as evidence that the monomer represented the biological

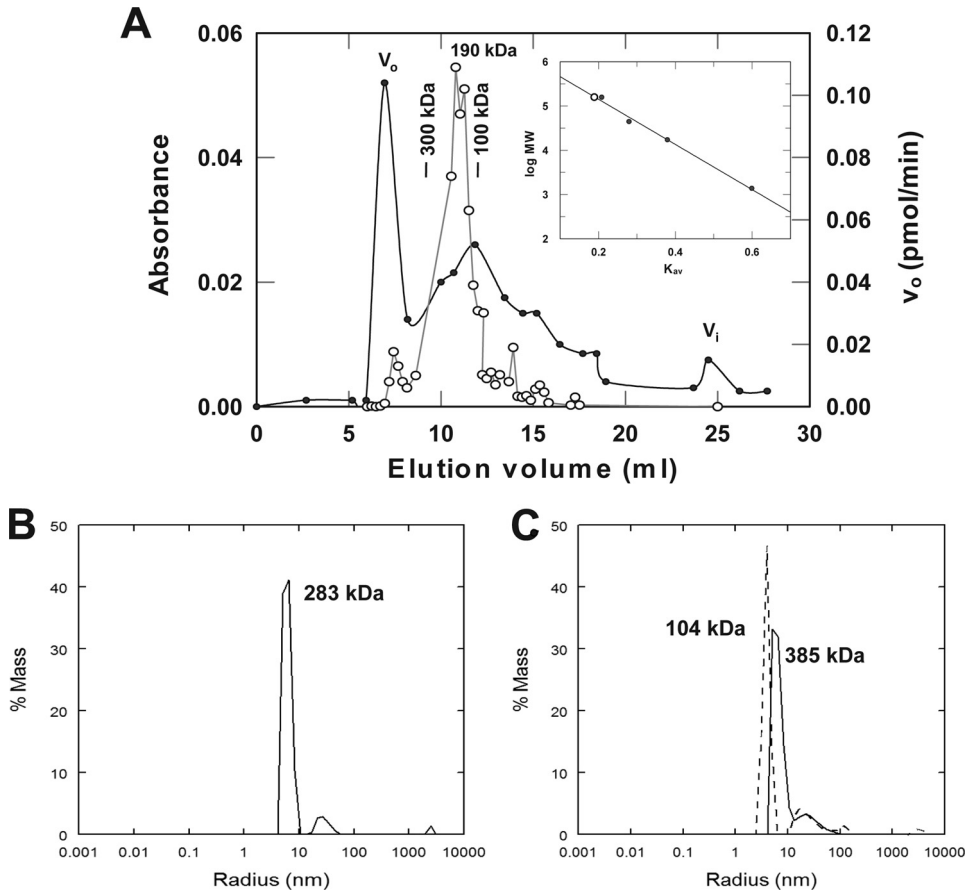

FIGURE 3. **Functional E6AP is an oligomer.** *A*, 150 μl of 75 μM full-length His_6-E6AP was analyzed in a 1× 30-cm Superose 12 FPLC gel filtration column equilibrated in 50 mM Tris-HCl (pH 7.5) and 50 mM NaCl. Protein was monitored by 280 nm absorbance (*filled circles*), and enzyme activity was monitored by E3-limiting ^{125}I-polyubiquitin chain formation (*open circles*). *Inset*, calibration plot with the elution position of the peak E6AP activity shown with an *open circle*. *B*, static light scattering analysis of 18 μM full-length His_6-E6AP in 50 mM Tris-HCl (pH 7.5) containing 200 mM NaCl at 37 °C as described under "Materials and Methods." The main peak of 283 kDa exhibits a polydispersity of 17%. The higher molecular weight low abundance peak of 50-nm radius represents residual aggregates not removed by Mono Q FPLC. *C*, static light scattering analysis identical to *A* in the presence of 16 μM His_6-E6AP and 8% (v/v) methanol in the absence (*solid line*; 23% polydispersity) or presence (*dashed line*; 14% polydispersity) of 61 mM Ac-$PheNH_2$.

relevant structure (49). However, we have recently demonstrated that the E6AP catalytic cycle comprises a two-step mechanism involving rapid transthiolation of activated ubiquitin from the cognate E2~ubiquitin co-substrate to the Hect Cys^{820} active site residue followed by rate-limiting chain elongation to form the polyubiquitin degradation signal (51). Because of this, Cys^{820} thioester formation is an insensitive measure of E6AP catalytic competence (51), accounting for the reported inconsistencies between known loss-of-function mutations in Angelman syndrome and retention of the ability of the enzyme to form an active Cys^{820}-linked thioester to ubiquitin (17). To re-examine this point, we mutated Phe^{727} to aspartic acid in order to more efficiently disrupt trimer formation. The E6APF727D mutation significantly ablates the ability of the enzyme to form polyubiquitin chains, as shown by the 62-fold decrease in k_{cat} without significant effect on the K_m for UbcH7~^{125}I-ubiquitin thioester binding (Table 2) or end point Cys^{820} thioester formation (not shown), the latter as noted previously (49).

As additional evidence that trimeric E6AP represents the functional form of the enzyme, we examined the effect of Ac-$PheNH_2$ as a mimic of Phe^{727}. The addition of Ac-$PheNH_2$ to His_6-E6AP results in quantitative dissociation of the oligomer to a 104 kDa peak in good agreement with the expected molecular weight of the monomer (Fig. 3*C*). This observation is consistent with substitution of Ac-$PheNH_2$ into the conserved hydrophobic pocket to disrupt the radially symmetric subunit interactions stabilizing the trimer and is accompanied by quantitative inhibition of ^{125}I-polyubiquitin chain formation (Fig. 4*D*). The dependence of initial velocity on $[UbcH7]_o$ in the absence or presence of 44 mM Ac-$PheNH_2$ shows the amino acid derivative to be a non-competitive inhibitor with a $K_i = 12 \pm 3$ mM, which is in good agreement with the calculated K_d of 27 mM predicted from the −2.13 kcal/mol stabilization predicted by PISA (see above). In addition, non-competitive inhibition by Ac-$PheNH_2$ is consistent with that predicted for an effect on subunit dissociation (Fig. 4*E*) and the observed consequence of the E6APF727D mutation (Table 2). Although Ac-$PheNH_2$ can potentially interact with other regions comprising the interface of full-length His_6-E6AP, the linearity of the double reciprocal plots for Fig. 4, *D* (*inset*) and *E*, are consistent with binding at a single homogeneous site, presumably the buried conserved hydrophobic pocket.

A Conserved α-Helix Blocks E6AP Trimer Formation—Examination of the extant structures for other Hect domains,

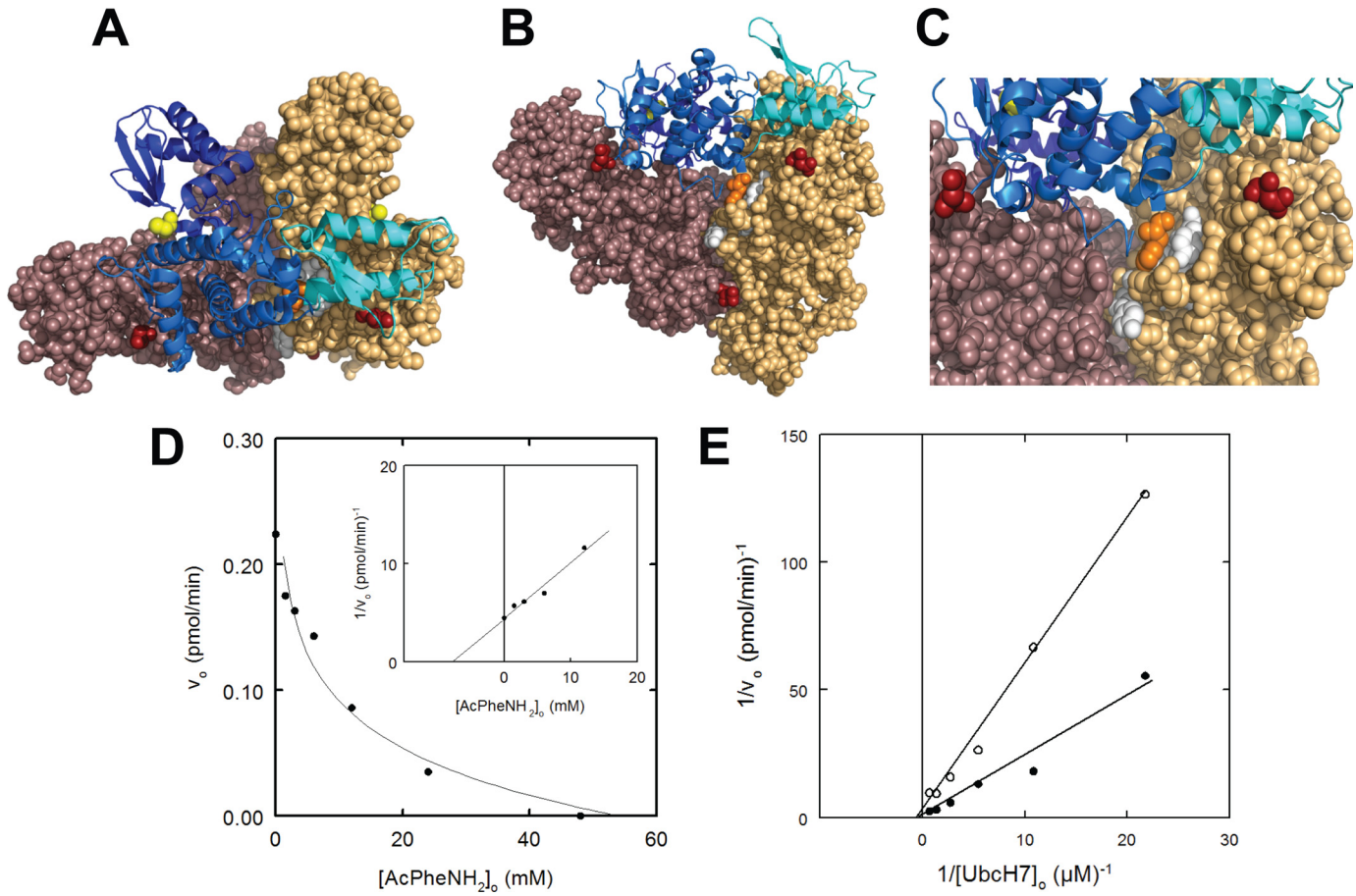

FIGURE 4. **Active E6AP is a trimer stabilized by Phe^{727} interactions.** *A*, structure of the E6AP Hect domain trimer (PDB code 1D5F) reported by Huang *et al.* (49). Each chain is *colored differently* to emphasize subunit packing, whereas the forward subunit is rendered as a *ribbon* and *colored* to distinguish the large N-terminal subdomain (*marine*), the small N-terminal subdomain (*cyan*), and the C-terminal subdomain (*dark blue*). The active site Cys^{820} and N-terminal residues are rendered in *CPK* and *colored yellow* and *red*, respectively. *B*, the structure of *A* is rotated 90° into the plane of the page to emphasize subunit packing. Residues of the hydrophobic pocket are rendered in *white* for the *gold* subunit, and Phe^{727} of the *blue* subunit is rendered in *orange*. *C*, closer view of Phe^{727} intercalated into the hydrophobic pocket of the adjacent subunit. *D*, the concentration dependence of Ac-PheNH$_2$ on the initial rate of ^{125}I-polyubiquitin chain assembly under E6AP-limiting conditions, with the *solid line* representing a nonlinear inverse regression analysis fit to a hyperbolic kinetics; *inset*, semireciprocal plot of the resulting data. Incubations contained 400 nM Uba1, 200 nM UbcH7, 8.8 nM His$_6$-E6AP, 5 μM ^{125}I-ubiquitin, and the indicated concentrations of Ac-PheNH$_2$. *E*, double reciprocal plot of the dependence of $[UbcH7]_o$ on the initial rate of polyubiquitin chain formation conducted as in *D* in the absence (*solid circles*) or presence (*open circles*) of 44 mM Ac-PheNH$_2$. All incubations contained 5% (v/v) methanol as a carrier for the Ac-PheNH$_2$.

TABLE 2
Summary of kinetic constants

	K_m	k_{cat}	k_{cat}/K_m
	nM	s^{-1}	$M^{-1}\,s^{-1}$
GST-E6AP-UbcH7[a]	58 ± 8	$3.1 \pm 0.9 \times 10^{-2}$	5.4×10^5
GST-E6APF727D-UbcH7[b]	72 ± 25	$5.0 \pm 0.7 \times 10^{-4}$	7.6×10^3
GST-E6APY533A-UbcH7	40 ± 12	$3.1 \pm 0.2 \times 10^{-3}$	7.9×10^4
GST-E6APD543A-UbcH7[b]	540 ± 400	$4.0 \pm 1.0 \times 10^{-3}$	7.5×10^3
GST-E6APR626A-UbcH7[b]	150 ± 50	$2.0 \pm 0.2 \times 10^{-4}$	1.3×10^3
GST-E6APK688A-UbcH7	39 ± 10	$5.2 \pm 0.4 \times 10^{-2}$	1.3×10^5

[a] From Table 1.
[b] The observed rates of these mutants approach our limit of detection for ^{125}I-polyubiquitin chain formation and result in a substantial increase in the S.E. of the measurements.

including WWP1 (PDB code 1ND7), Smurf2 (PDB code 1ZVD), HuWE1 (PDB code 3H1D), Nedd4-1 (PDB code 2XBB), Nedd4-2 (PDB code 2XBF), and yeast RSP5 (PDB codes 3OLM and 4LCD), provides no other instance of trimer formation (69–73). However, the other Hect domain structures contain additional sequence N-terminal to the truncation site for E6AP at Asn^{497} that is not present in the E6AP structure (49). Immediately N-terminal to Asn^{497} is an extensive amphipathic α-helix corresponding to residues 474–490 that is relatively conserved among the Hect ligases, contributes to domain stability, and correlates with reduced autoubiquitination and target protein conjugation (71, 74). In all of the Hect domain structures containing the additional segment, the hydrophobic face of the amphipathic N-terminal α-helix binds to the hydrophobic pocket normally occupied by Phe^{727} in the trimeric E6AP structure (69–73). We speculate that the latter interaction of the α-helix might block oligomerization, accounting for the observed reduction in ligase activity because we here demonstrate that trimer formation is required for polyubiquitin chain assembly. To address the role of the N-terminal α-helix, the initial rate of polyubiquitin chain formation was analyzed in the absence or presence of an N-terminal blocked Ac-NRIRMYSERRITVLYSL peptide corresponding to residues 474–490 of E6AP isoform 1 to mimic the proposed effect of this segment (Fig. 5). With increasing concentrations of the peptide, the initial rate of E6AP-catalyzed chain formation decreased with a hyperbolic dependence (Fig. 5*A*), as shown by the linearity of the corresponding semireciprocal plot, yielding an apparent K_i of 22 ± 2 μM (Fig. 5*A*, *inset*).

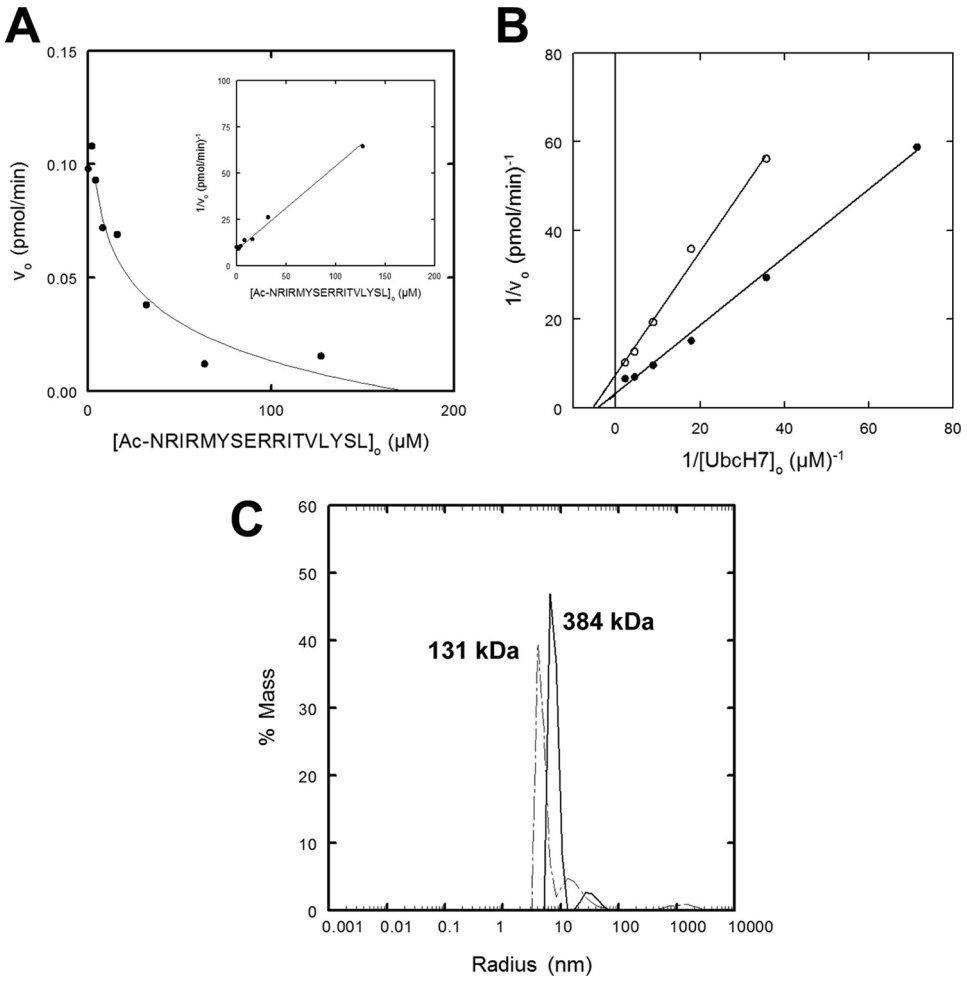

FIGURE 5. **The N-terminal α-helical peptide inhibits E6AP ligase function.** *A*, initial rates of ^{125}I-polyubiquitin chain assembly under E6AP-limiting conditions were analyzed in the absence or presence of the indicated concentrations of N-terminal peptide and evaluated by nonlinear regression fit to an inverse hyperbolic equation. Reactions contained 34 nM Uba1, 390 nM UbcH7, 1.3 nM His$_6$-E6AP, and 4 μM ^{125}I-ubiquitin. *Inset*, semireciprocal plot of the data. *B*, double reciprocal plot of initial rates of ^{125}I-polyubiquitin chain assembly under E6AP-limiting conditions in the absence (*closed circles*) or presence (*open circles*) of 32 μM N-terminal peptide. Reactions contained 33 nM Uba1, 0.6 nM His$_6$-E6AP, 4 μM ^{125}I-ubiquitin, and the corresponding [UbcH7]$_o$ concentrations. *C*, the static light scattering spectrum of 17 μM full-length His$_6$-E6AP was determined as described in the legend to Fig. 3*C* in the absence (*solid line*; 10 ± 3% polydispersity) or presence (*dashed line*; 10 ± 2% polydispersity) of 88 μM Ac-NRIRMYSERRITVLYSL peptide.

When the concentration dependence of the initial rate for polyubiquitin chain formation on [UbcH7]$_o$ was examined in the absence or presence of 32 μM peptide, the isolated α-helix was a classic non-competitive inhibitor (Fig. 5*B*). The empirical K_i probably underestimates the intrinsic affinity of the wild type N-terminal α-helix because the isolated peptide is unlikely quantitatively to maintain the secondary structure of the intact protein. Nonetheless, observation of non-competitive inhibition is consistent with the peptide blocking trimerization of E6AP in a manner analogous to Ac-PheNH$_2$ (Fig. 4, *D* and *E*) and mutation of Phe^{727} (Table 2). Further, the peptide promotes dissociation of the E6AP oligomer when analyzed by static light scattering (Fig. 5*C*).

Identification of Additional Subunit Interface Residues Affecting E6AP Catalytic Activity—The present data and recent insights into the properties of protein subunit interfaces support the E6AP trimer as the catalytically relevant structure (67, 68). The interaction surfaces of the trimer were analyzed by PISA to define other side chain interactions contributing to stability beyond that of Phe^{727} (supplemental Table 1). A comprehensive sequence alignment of human Hect ligases cross-referenced to the results of PISA identified a number of conserved positions that appear potentially critical, including the hydrophobic pocket residues into which Phe^{727} intercalates, as discussed earlier. Interestingly, several of these residues represent or are adjacent to documented Angelman syndrome point mutations. We were particularly interested in Tyr^{533}, which is an Angelman syndrome mutation site and which participates in a pattern of side chain interactions between subunits (75). Tyrosine 533 also exists in the region of subunit interface recently suggested by Chan *et al.* to be sensitive to cAbl-dependent regulation by phosphorylation of Tyr^{636} (76).

For two of the subunits in the trimer structure, the side chain phenolic group of Tyr^{533} hydrogen bonds with the amide hydrogen of Asp^{543} present on the same polypeptide chain (Fig. 6*B*), whereas for the third subunit, Tyr^{533} is rotated 60° and hydrogen-bonds to the amide hydrogens of Arg^{626} and Thr^{624} on the adjacent chain (Fig. 6*C*). More important, for all three subunits, the side chain carboxyl and amide carbonyl groups of

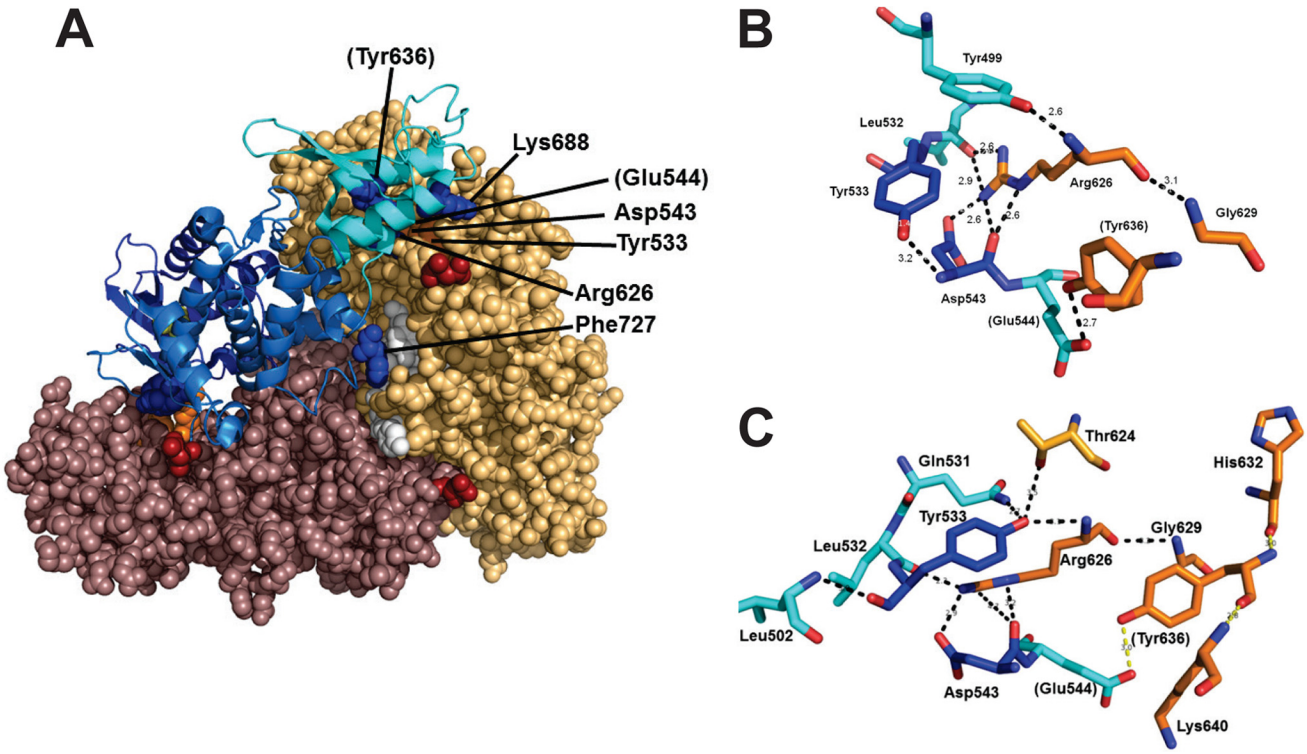

FIGURE 6. **Selected side chain interactions within the E6AP Hect domain trimer.** *A*, structure of the E6AP Hect domain trimer portrayed in Fig. 4*B* illustrating additional residues stabilizing the structure. *B* and *C*, *close-up views* of the spatial orientation for Tyr^{533}, Asp^{543}, and Arg^{626}. Subunit residues are *color-coded* like those in *A*. Residues in *parentheses* are those previously examined by Chan *et al.* (76).

Asp^{543} hydrogen-bond to the side chain guanidinium of Arg^{626} (Fig. 6, *B* and *C*). Tyrosine 533 and Asp^{543} reside within the Hect large N-terminal subdomain, whereas Arg^{626} is in the small N-terminal subdomain of the adjacent subunit, so that the three residues constitute a radial symmetric pattern of subunit interactions. We independently mutated each of the residues to alanine and examined the effect on the kinetics for ^{125}I-polyubiquitin chain formation with respect to [UbcH7]$_o$ under rigorously E3-limiting conditions (Table 2). As a control, we similarly also mutated Lys^{688}, a residue present on the same small N-terminal subdomain interface as Arg^{626}, which PISA analysis indicates hydrogen-bonds to the side chain of Glu^{535} in the adjacent subunit. All four mutants formed ^{125}I-ubiquitin thioesters to Cys^{820} with kinetics qualitatively similar to that of wild type enzyme in short term incubations described previously (51).

Mutation of Lys^{688} did not have a significant effect on the kinetics of ^{125}I-polyubiquitin chain assembly (Table 2). However, given the large number of predicted subunit interactions stabilizing the trimer (supplemental Table 1), abrogating a single site might not be expected *a priori* to have a large effect except for those interactions particularly critical for structural integrity. In contrast to the effect of mutating Tyr^{688}, mutation of Tyr^{533} decreased k_{cat} 10-fold but had no effect on the K_m for UbcH7~ubiquitin binding (Table 2). Similarly, mutation of Arg^{626} decreased k_{cat} 155-fold but had little effect on K_m (Table 2). Both of the latter mutants are consistent with an effect on oligomerization, given their position within the trimer structure and distance from the active site Cys^{820} as well as the fact that neither mutation alters the ability of E6AP to bind its UbcH7~ubiquitin thioester substrate. Mutation of Asp^{543} similarly ablated k_{cat} 8-fold but additionally increased K_m significantly (Table 2). Together with the effects of Tyr^{636} phosphorylation (76), the consequences of these point mutants reveal complex interactions affecting the catalytic function of E6AP.

E6 Protein Enhances E6AP Polyubiquitin Chain Synthesis—HPV16 E6 protein is thought to promote viral replication and host epithelial cell transformation by serving as an E6AP adapter to target the p53 tumor suppressor protein for 26 S proteasome-dependent degradation (32, 77, 78). Recent structural work demonstrates that the 158-amino acid E6 viral protein contains structurally related N-terminal and C-terminal Zn^{2+} binding domains connected by a linker polypeptide (46). The C-terminal domain binds p53 but also shows limited interaction with E6AP (43, 79). In contrast, the N-terminal domain exhibits significant affinity for E6AP through binding to a canonical L*XX*LL motif on the ligase and is additionally responsible for E6 protein self-association (40–42, 46), accounting for the observation that the complex between E6 protein and p53 consists of a p53 tetramer and an E6 dimer (45, 80). As expected, disrupting the dimerization interface by mutation inhibits E6-dependent p53 conjugation by E6AP but also enhances E6 protein solubility (46), which probably relates to earlier observations that ectopic expression of E6 protein stimulates autoubiquitination and subsequent E6AP degradation *in vivo* (81).

Because the trimer is the presumed catalytically fully active form of E6AP, we speculated that the effect of E6 protein on E6AP turnover (82) and the stabilization of p53 when the E6 dimerization interface is disrupted might reflect the ability of

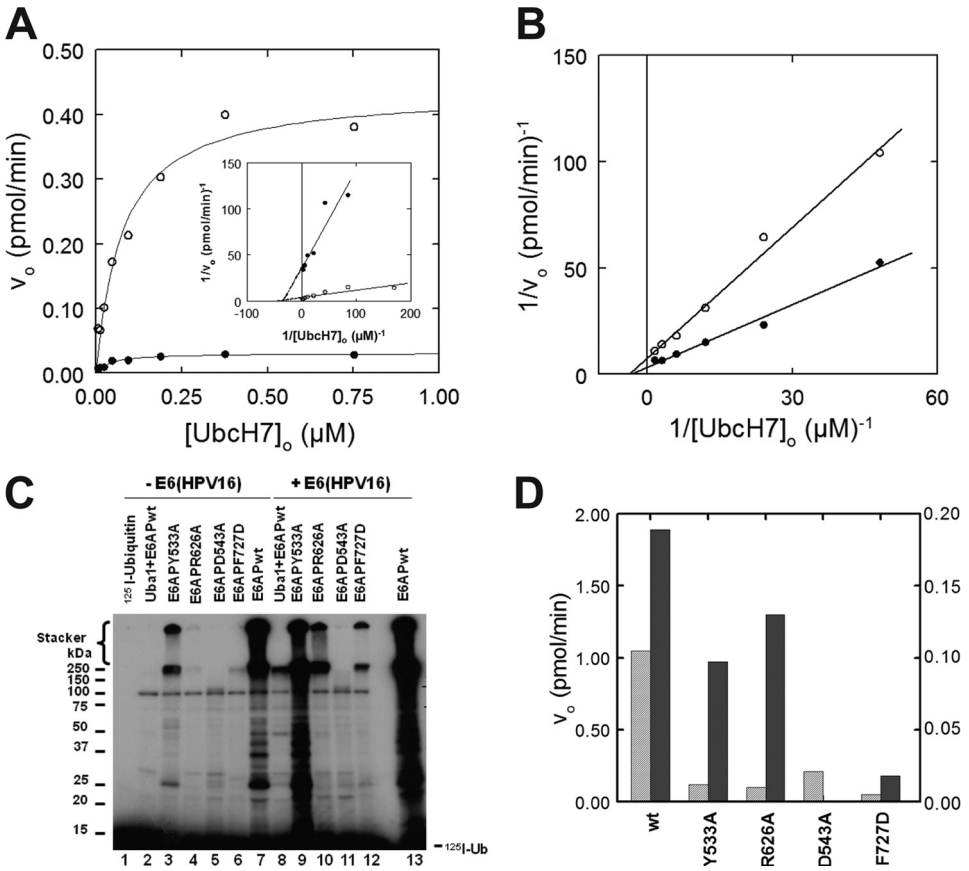

FIGURE 7. **E6 protein enhances E6AP ligase activity and rescues selected Angelman syndrome mutations.** *A*, initial rates of ^{125}I-ubiquitin polyubiquitin chain formation were determined under E6AP-limiting conditions in the absence (*closed circles*) or presence (*open circles*) of 20 nM E6 protein as described under "Material and Methods" and evaluated by nonlinear regression fit to the Michaelis-Menten equation. Assays contained 70 nM Uba1, 0.4 nM His-E6AP, 4 μM ^{125}I-ubiquitin, and the indicated UbcH7 concentrations. *Inset*, double reciprocal plot of the data. *B*, double reciprocal plot of the initial rates of ^{125}I-ubiquitin conjugation activity determined under E6AP-limiting conditions in the absence (*closed circles*) or presence (*open circles*) of 3.3 μM E6 (HPV16)Δ91, as described under "Materials and Methods" and in *A*. Assays contained 30 nM Uba1, 1 nM His$_6$-E6AP, 4 μM ^{125}I-ubiquitin, and the indicated UbcH7 concentrations. *C*, conjugation reactions similar to those of *B* were conducted with 110 nM Uba1, 480 nM UbcH7, 5 μM ^{125}I-ubiquitin, and 1 nM wild type or mutant GST-E6AP in the absence (*lanes 1–7*) or presence (*lanes 8–13*) of 20 nM E6(HPV16). *D*, quantitation of product formation rates from *C* in the absence (*light gray*) or presence (*dark gray*) of E6(HPV16). Data for wild type GST-E6AP and GST-E6APY533A are plotted on the *left axis*, whereas data for GST-E6APR626A, -D543A, and -F727D are plotted on the *right axis*.

the viral protein to promote E6AP oligomerization. Fig. 7*A* shows the effect of recombinant E6 protein on the [UbcH7]$_o$ dependence of E6AP-catalyzed ^{125}I-polyubiquitin chain formation. Initial rates of chain formation were significantly enhanced in the presence of E6 protein, with the k_{cat} increasing from 0.057 $\pm$ 0.029 s^{-1} in the absence of E6 protein to 0.81 $\pm$ 0.045 s^{-1} in its presence. The corresponding double reciprocal plot shows E6 protein to be a nonessential activator, exhibiting a k_{cat} effect (*inset*), and with a K_d for E6 binding corresponding to 1.5 nM. These results are consistent with a mechanism in which the E6 dimer promotes oligomerization of E6AP to the catalytically competent trimer through binding to a site distinct from the catalytic site, presumably the leucine-rich L*XX*LL motif (40–42). Although the N-terminal domain contains both the dimerization interface and the L*XX*LL association motif (46), the recombinant E6(HPV16)Δ91 N-terminal domain encompassing residues 1–91 (46) inhibits E6AP-catalyzed polyubiquitin chain formation with a hyperbolic concentration dependence (apparent $K_i = 4$ μM; not shown) and displays non-competitive inhibition with respect to [UbcH7]$_o$, corresponding to $K_i = 6$ μM (Fig. 7*B*). Similarly, the recombinant E6(HPV16)Ct C-terminal domain encompassing residues 89–158 is a non-competitive inhibitor of E6AP with respect to [UbcH7]$_o$ corresponding to $K_i = 4$ μM (not shown). Collectively, the results indicate that both E6 domains bind E6AP, presumably at different sites, to promote oligomerization of full-length E6AP. This conclusion supports earlier empirical binding evidence demonstrating interaction of each domain with E6AP (44, 46).

Because full-length E6 protein acts as a nonessential activator, presumably by promoting E6AP trimer formation, we asked whether the viral protein could rescue the loss-of-function phenotype displayed by the E6APF727D point mutant. The addition of 20 nM E6 protein significantly enhanced the initial rate of ^{125}I-polyubiquitin chain formation for wild type protein (Fig. 7*C*, *lanes 7* and *13*) as seen in Fig. 7*A* and E6APF727D (Fig. 7*C*, *lanes 6* and *12*). Similar rescue of ^{125}I-polyubiquitin chain formation was observed in an 8-fold increase in rate for E6APY533A (Fig. 7*C*, *lanes 3* and *9*) and a 13-fold increase in rate for E6APR626A (Fig. 7*C*, *lanes 4* and *10*). In contrast, no enhancement in rate was observed for the E6APD543A point mutant (Fig. 7*C*, *lanes 5* and *11*). These results are consistent with E6 rescuing the

loss-of-function phenotype for selected point mutants by promoting oligomerization.

DISCUSSION

Homo- and hetero-oligomerization regulate many complex biochemical processes in the cell (83), and recent findings suggest that such protein interactions are critical for the mechanism(s) of assembling polyubiquitin signals during key events of cell regulation (52, 84–88). The present studies were prompted in part by our attempt to explicate the puzzling observation that the assembly of ^{125}I-polyubiquitin chains by GST-E6AP is ablated when the affinity tag is removed following digestion with thrombin. Subsequent experiments indicated that the ability of GST to dimerize (64–66) promotes oligomerization of E6AP, confirmed by the quantitative inhibition of ligase-catalyzed chain formation by free GST, GST-E6APΔ495, and GST-E6APC820A (Fig. 1). The ability of thrombin-processed E6APΔ495 and E6APC820A to similarly inhibit wild type GST-E6AP polyubiquitin chain formation demonstrates that oligomerization is an intrinsic property of the Hect ligase, with the interaction interfaces probably spanning the N-terminal targeting and C-terminal Hect domains of the ligase (Fig. 1). In addition, co-purification of recombinant baculovirally expressed His_6-E6AP with full-length E6AP lacking the His_6 affinity tag is consistent with oligomerization of the ligase (Fig. 2*B*). The progressive increase in k_{cat} for E6AP-catalyzed ^{125}I-polyubiquitin chain assembly with the absence of competing degradative fragments is consistent with a role for oligomerization in the activity of E6AP (Table 1). Finally, static light scattering measurements are consistent with the homotrimer as the catalytically relevant form of E6AP (Fig. 3).

Trimeric E6AP was initially dismissed as an artifact of crystal packing forces, particularly because a F727A point mutant capable of disrupting the oligomer did not affect the ability of the enzyme to catalyze transthiolation from E2~ubiquitin thioester (49); however, more comprehensive functional assays were unavailable for testing additional potential effects of trimer disruption. In the present studies, we demonstrate that a paralogous F727D mutation intended to more completely disrupt trimer formation significantly ablates the ability of the enzyme to catalyze elongation of polyubiquitin chains to <2% of wild type enzyme (Table 2), concomitant with dissociation of the oligomer (Fig. 3). As noted previously for the F727A mutant (89), mutation of Phe^{727} to aspartic acid has no effect on formation of the essential Cys^{820}~ubiquitin thioester intermediate (not shown). *In silico* PISA analysis of the subunit interfaces present within the E6AP trimer identifies a cohort of conserved residues within the 7508 Å^2 buried by oligomerization (supplemental Fig. 1*A*). Of the significant number of hydrogen bond and salt bridge interactions identified by PISA (supplemental Table 1), the conserved radially symmetric network of interactions represented by the intersubunit intercalation of Phe^{727} into the hydrophobic pocket present on the adjacent subunit appears particularly important because mutation of Phe^{727} or antagonizing the interaction by the addition of Ac-PheNH_2 disrupts trimer formation and significantly ablates activity (Fig. 4). The linearity of the double reciprocal plots in the presence of Ac-PheNH_2 (Fig. 4, *D* and *E*) and the good agreement between the empirical K_i of 12 mM and the value of 27 mM predicted from the calculated binding energy of Phe^{727} (−2.13 kcal/mol) are consistent with the amino acid derivative binding at the unique hydrophobic pocket present in the subunit interface.

Among the extant structures for Hect domains, that of E6AP is unique in forming a trimer (69–73). The 1DF5 E6AP trimer is also notable in being the only such Hect domain structure lacking the additional N-terminal sequence segment present in the other paralogs. In the other structures, a conserved α-helix within this sequence binds to the hydrophobic pocket otherwise occupied by Phe^{727} in the E6AP trimer (69–73). We demonstrate that E6AP residues 474–490, corresponding to the α-helical region, act as a non-competitive inhibitor of ^{125}I-polyubiquitin chain formation with an affinity ($K_i = 22 \pm 2$ μM) considerably greater than that of Ac-PheNH_2 ($K_i = 12 \pm 3$ mM) (Fig. 5). The presence of the additional α-helical segment is reported to enhance the intrinsic stability of the Hect domain and to ablate autoubiquitination (71, 74). The latter has been interpreted as demonstrating a regulatory role for the interaction between the α-helical segment and the hydrophobic pocket in the native full-length structure. Although we cannot *a priori* rule out such a regulatory role for the α-helix, we propose that association of the α-helical segment with the hydrophobic pocket is a structural artifact of the position of the truncation for the other Hect domain constructs and predict that in the absence of this interaction, the other ligases would assume a trimeric structure analogous to that of E6AP. We note as well that in the absence of trimer formation, packing of the Hect domains within the unit cells influences the orientation of the C-terminal domain, altering their positions relative to the large N-terminal subdomains (69–73). The various positions observed for the C-terminal domains in different Hect domain structures have been previously interpreted to reflect the requirement for flexibility during the catalytic cycle of the enzyme, suggested by the ablation of activity accompanying mutations in the linker region connecting the C-terminal and large N-terminal subdomains (69, 73, 82). We suggest, instead, that these alternate orientations for the C-terminal domain may reflect artifactual crystal packing forces present in the absence of trimerization.

A second subunit interface identified as important for trimer activity localizes to interactions among Tyr^{533} and Asp^{543}, within the large N-terminal subdomain, and the small N-terminal subdomain residue Arg^{626} (76) of the adjacent subunit (Fig. 6). These residues form a network of hydrogen-bonded interactions that appear to stabilize the trimer because individual mutation of each significantly affects k_{cat} but with little consequence for UbcH7~ubiquitin thioester binding (Table 2). The functional effects of these mutations collectively support the trimer as the catalytically relevant structure for E6AP. Mutation of Asp^{543} appears to be the single exception because its mutation affects both k_{cat} and binding of the UbcH7~ubiquitin thioester substrate (Table 2). The latter may reflect a structural contribution for the side chain interactions of Asp^{543} or the special role for the residue in bridging the effects of Tyr^{533} and Arg^{626} (Fig. 6), which makes its mutation equivalent to a double mutant. In contrast, disrupting the hydrogen bond between

Lys^{688} in the small N-terminal subdomain and Glu^{535} in the adjacent large N-terminal subdomain by mutation of the former has no consequence, indicating that the effects of the previous mutations are specific to those residues rather than a general feature of the interface. Interestingly, this subunit interface harbors Tyr^{636}, which Chan *et al.* (76) have identified as a substrate for c-Abl phosphorylation in the regulation of E6AP function. Chan *et al.* (76) have speculated that the inhibition of E6AP activity observed on phosphorylation of Tyr^{636} might result from blocking oligomerization of the enzyme. Our empirical observations and the effect of mutation on other residues within this region support a role for Tyr^{636} in regulating trimer formation and E6AP activity.

The ability of E6 protein to recruit p53 to E6AP for targeted degradation is the accepted paradigm by which HPV-16 transforms infected epithelial cells (32, 77, 78). Structural studies demonstrating dimerization of E6 protein have more recently accounted for the observed stoichiometry of the resulting $E6_2$-$p53_4$ complex (45, 80). Given our observation that oligomeric E6AP is the catalytically competent form of the ligase, we asked whether the ability of E6 protein to dimerize could promote E6AP-catalyzed polyubiquitin chain formation. The data of Fig. 7 demonstrate that E6 protein is a potent nonessential activator of E6AP catalytic activity within a low nanomolar concentration range ($K_{activation}$ = 1.5 nM). The $K_{activation}$ for ligase stimulation, representing the binding of E6 to E6AP, is significantly lower than the 4 μM K_d for binding of the viral protein to E6AP reported previously by surface plasmon resonance (44), probably reflecting the enhanced entropically coupled affinity associated with binding to linked sites (90). The latter indicates that E6 protein probably functions at intracellular concentrations significantly lower than suggested by the isolated *in vitro* equilibrium binding affinity. In the absence of substrate, E6AP catalyzes the assembly of free and anchored polyubiquitin chains, the latter attached to the ligase through autoubiquitination (51). This bifurcation of products is proposed to occur by partitioning of a Cys^{820}~polyubiquitin intermediate between transfer to water or a lysine present on the ligase, respectively (51). The addition of E6 protein uniformly enhances the formation of both ^{125}I-polyubiquitin products, consistent with the partitioning model (Fig. 7*C*). The latter observation explains the earlier observation that ectopic expression of E6 protein stimulates the autoubiquitination and degradation of endogenous E6AP (48). More importantly, these observations anticipate that E6 protein-dependent epithelial cell transformation may arise in part through a general stimulation of ligase activity toward its normal cohort of endogenous targets rather than serving exclusively as a binding adapter to target a small subset of alternate targets, such as p53 (Fig. 7*A*). Such a proposal is consistent with earlier observations that an E6 SAT_{8-10} mutant defective in targeting E6AP-dependent p53 degradation (48) but retaining the ability to immortalize human epithelial cells, induce colony growth on soft agar, and stimulate telomerase activity (84, 86) also simulates E6AP autoubiquitination and degradation *in vitro* (48).

The 14-fold stimulation in E6AP activity at saturating E6 protein suggests that only 0.7% of the active ligase, determined by stoichiometric Cys^{820}~^{125}I-ubiquitin thioester formation, is present as the active trimer under the conditions of Fig. 7*A*, although we cannot rule out an intermediate level of activity from potential dimeric species derived from the trimeric structure. Consistent with the remarkable effect of E6 in promoting oligomerization, the viral protein complements the kinetic phenotypes resulting from the F727D, R626A, and Y533A mutations, the latter being a documented Angelman syndrome mutation site (75). Because the F727D mutation results from defective trimer formation, functional complementation of the R626A and Y533A mutations suggests that they as well represent trimer formation defects.

The present observations significantly extend our understanding of the underlying mechanism of the E6AP catalytic cycle and that of the Hect domain superfamily. Identification of oligomeric E6AP, presumably as the trimer or multiples thereof, as the catalytically relevant form of the ligase explains a number of previous observations in the literature and reveals potential pharmacological approaches to modulate activity of the enzyme. Accordingly, Ac-PheNH_2 serves as an important proof of principle lead compound for potential future E6AP antagonists targeted to the disruption of oligomerization. Similarly, E6 protein suggests as yet unidentified cellular mechanisms modulating E6AP oligomerization that could serve as additional therapeutic targets. Finally, these observations emphasize the importance of quantitative biochemically defined studies unambiguously defining the mechanism of the ubiquitin ligases.

REFERENCES

1. Huibregtse, J. M., Scheffner, M., Beaudenon, S., and Howley, P. M. (1995) A family of proteins structurally and functionally related to the E6-AP ubiquitin-protein ligase. *Proc. Natl. Acad. Sci. U.S.A.* **92,** 2563–2567
2. Rotin, D., and Kumar, S. (2009) Physiological functions of the HECT family of ubiquitin ligases. *Nat. Rev. Mol. Cell Biol.* **10,** 398–409
3. Wang, M., and Pickart, C. M. (2005) Different HECT domain ubiquitin ligases employ distinct mechanisms of polyubiquitin chain synthesis. *EMBO J.* **24,** 4324–4333
4. Wang, M., Cheng, D., Peng, J., and Pickart, C. M. (2006) Molecular determinants of polyubiquitin linkage selection by an HECT ubiquitin ligase. *EMBO J.* **25,** 1710–1719
5. Beaudenon, S., and Huibregtse, J. M. (2008) HPV E6, E6AP and cervical cancer. *BMC Biochem.* **9,** S4
6. Flashner, B. M., Russo, M. E., Boileau, J. E., Leong, D. W., and Gallicano, G. I. (2013) Epigenetic factors and autism spectrum disorders. *Neuromolecular Med.* **15,** 339–350
7. Nicholls, R. D., and Knepper, J. L. (2001) Genome organization, function, and imprinting in Prader-Willi and Angelman syndromes. *Annu. Rev. Genomics Hum. Genet.* **2,** 153–175
8. Matentzoglu, K., and Scheffner, M. (2008) Ubiquitin ligase E6-AP and its role in human disease. *Biochem. Soc. Trans.* **36,** 797–801
9. Kishino, T., Lalande, M., and Wagstaff, J. (1997) UBE3A/E6-AP mutations cause Angelman syndrome. *Nat. Genet.* **15,** 70–73
10. Sutcliffe, J. S., Jiang, Y. H., Galijaard, R. J., Matsuura, T., Fang, P., Kubota, T., Christian, S. L., Bressler, J., Cattanach, B., Ledbetter, D. H., and Beaudet, A. L. (1997) The E6-Ap ubiquitin-protein ligase (UBE3A) gene is localized within a narrowed Angelman syndrome critical region. *Genome Res.* **7,** 368–377
11. Mabb, A. M., Judson, M. C., Zylka, M. J., and Philpot, B. D. (2011) Angelman syndrome. Insights into genomic imprinting and neurodevelopmental phenotypes. *Trends Neurosci.* **34,** 293–303
12. Matsuura, T., Sutcliffe, J. S., Fang, P., Galjaard, R. J., Jiang, Y. H., Benton, C. S., Rommens, J. M., and Beaudet, A. L. (1997) *De novo* truncating mutations in E6-AP ubiquitin-protein ligase gene (UBE3A) in Angelman syn-

drome. *Nat. Genet.* **15,** 74–77
13. Lossie, A. C., Whitney, M. M., Amidon, D., Dong, H. J., Chen, P., Theriaque, D., Hutson, A., Nicholls, R. D., Zori, R. T., Williams, C. A., and Driscoll, D. J. (2001) Distinct phenotypes distinguish the molecular classes of Angelman syndrome. *J. Med. Genet.* **38,** 834–845
14. Williams, C. A., Beaudet, A. L., Clayton-Smith, J., Knoll, J. H., Kyllerman, M., Laan, L. A., Magenis, R. E., Moncla, A., Schinzel, A. A., Summers, J. A., and Wagstaff, J. (2006) Angelman syndrome 2005. Updated consensus for diagnostic criteria. *Am. J. Med. Genet. A* **140,** 413–418
15. Clayton-Smith, J., and Laan, L. (2003) Angelman syndrome. A review of the clinical and genetic aspects. *J. Med. Genet.* **40,** 87–95
16. Jiang, Y., Lev-Lehman, E., Bressler, J., Tsai, T. F., and Beaudet, A. L. (1999) Genetics of Angelman syndrome. *Am. J. Hum. Genet.* **65,** 1–6
17. Cooper, E. M., Hudson, A. W., Amos, J., Wagstaff, J., and Howley, P. M. (2004) Biochemical analysis of Angelman syndrome-associated mutations in the E3 ubiquitin ligase E6-associated protein. *J. Biol. Chem.* **279,** 41208–41217
18. Smith, S. E., Zhou, Y. D., Zhang, G., Jin, Z., Stoppel, D. C., and Anderson, M. P. (2011) Increased gene dosage of Ube3a results in autism traits and decreased glutamate synaptic transmission in mice. *Sci. Transl. Med.* **3,** 103ra97
19. Schaaf, C. P., Sabo, A., Sakai, Y., Crosby, J., Muzny, D., Hawes, A., Lewis, L., Akbar, H., Varghese, R., Boerwinkle, E., Gibbs, R. A., and Zoghbi, H. Y. (2011) Oligogenic heterozygosity in individuals with high-functioning autism spectrum disorders. *Hum. Mol. Genet.* **20,** 3366–3375
20. Glessner, J. T., Wang, K., Cai, G., Korvatska, O., Kim, C. E., Wood, S., Zhang, H., Estes, A., Brune, C. W., Bradfield, J. P., Imielinski, M., Frackelton, E. C., Reichert, J., Crawford, E. L., Munson, J., Sleiman, P. M., Chiavacci, R., Annaiah, K., Thomas, K., Hou, C., Glaberson, W., Flory, J., Otieno, F., Garris, M., Soorya, L., Klei, L., Piven, J., Meyer, K. J., Anagnostou, E., Sakurai, T., Game, R. M., Rudd, D. S., Zurawiecki, D., McDougle, C. J., Davis, L. K., Miller, J., Posey, D. J., Michaels, S., Kolevzon, A., Silverman, J. M., Bernier, R., Levy, S. E., Schultz, R. T., Dawson, G., Owley, T., McMahon, W. M., Wassink, T. H., Sweeney, J. A., Nurnberger, J. I., Coon, H., Sutcliffe, J. S., Minshew, N. J., Grant, S. F., Bucan, M., Cook, E. H., Buxbaum, J. D., Devlin, B., Schellenberg, G. D., and Hakonarson, H. (2009) Autism genome-wide copy number variation reveals ubiquitin and neuronal genes. *Nature* **459,** 569–573
21. Samaco, R. C., Hogart, A., and LaSalle, J. M. (2005) Epigenetic overlap in autism-spectrum neurodevelopmental disorders. MECP2 deficiency causes reduced expression of UBE3A and GABRB3. *Hum. Mol. Genet.* **14,** 483–492
22. Yashiro, K., Riday, T. T., Condon, K. H., Roberts, A. C., Bernardo, D. R., Prakash, R., Weinberg, R. J., Ehlers, M. D., and Philpot, B. D. (2009) Ube3a is required for experience-dependent maturation of the neocortex. *Nat. Neurosci.* **12,** 777–783
23. Sato, M., and Stryker, M. P. (2010) Genomic imprinting of experience-dependent cortical plasticity by the ubiquitin ligase gene Ube3a. *Proc. Natl. Acad. Sci. U.S.A.* **107,** 5611–5616
24. Huang, H. S., Burns, A. J., Nonneman, R. J., Baker, L. K., Riddick, N. V., Nikolova, V. D., Riday, T. T., Yashiro, K., Philpot, B. D., and Moy, S. S. (2013) Behavioral deficits in an Angelman syndrome model. Effects of genetic background and age. *Behav. Brain Res.* **243,** 79–90
25. Greer, P. L., Hanayama, R., Bloodgood, B. L., Mardinly, A. R., Lipton, D. M., Flavell, S. W., Kim, T. K., Griffith, E. C., Waldon, Z., Maehr, R., Ploegh, H. L., Chowdhury, S., Worley, P. F., Steen, J., and Greenberg, M. E. (2010) The Angelman Syndrome protein Ube3A regulates synapse development by ubiquitinating arc. *Cell* **140,** 704–716
26. Margolis, S. S., Salogiannis, J., Lipton, D. M., Mandel-Brehm, C., Wills, Z. P., Mardinly, A. R., Hu, L., Greer, P. L., Bikoff, J. B., Ho, H. Y., Soskis, M. J., Sahin, M., and Greenberg, M. E. (2010) EphB-mediated degradation of the RhoA GEF Ephexin5 relieves a developmental brake on excitatory synapse formation. *Cell* **143,** 442–455
27. Gregianin, E., Vazza, G., Scaramel, E., Boaretto, F., Vettori, A., Leonardi, E., Tosatto, S. C., Manara, R., Pegoraro, E., and Mostacciuolo, M. L. (2013) A novel SACS mutation results in non-ataxic spastic paraplegia and peripheral neuropathy. *Eur. J. Neurol.* **20,** 1486–1491
28. Dagli, A., Buiting, K., and Williams, C. A. (2012) Molecular and clinical aspects of Angelman syndrome. *Mol. Syndromol.* **2,** 100–112
29. Philpot, B. D., Thompson, C. E., Franco, L., and Williams, C. A. (2011) Angelman syndrome. Advancing the research frontier of neurodevelopmental disorders. *J. Neurodev. Disord.* **3,** 50–56
30. Kühnle, S., Mothes, B., Matentzoglu, K., and Scheffner, M. (2013) Role of the ubiquitin ligase E6AP/UBE3A in controlling levels of the synaptic protein Arc. *Proc. Natl. Acad. Sci. U.S.A.* **110,** 8888–8893
31. Scheffner, M., Huibregtse, J. M., Vierstra, R. D., and Howley, P. M. (1993) The HPV-16 E6 and E6-AP complex functions as a ubiquitin-protein ligase in the ubiquitination of p53. *Cell* **75,** 495–505
32. Huibregtse, J. M., Scheffner, M., and Howley, P. M. (1991) A cellular protein mediates association of p53 with the E6 oncoprotein of human papillomavirus types 16 or 18. *EMBO J.* **10,** 4129–4135
33. Beer-Romero, P., Glass, S., and Rolfe, M. (1997) Antisense targeting of E6AP elevates p53 in HPV-infected cells but not in normal cells. *Oncogene* **14,** 595–602
34. Haupt, Y., Maya, R., Kazaz, A., and Oren, M. (1997) Mdm2 promotes the rapid degradation of p53. *Nature* **387,** 296–299
35. Talis, A. L., Huibregtse, J. M., and Howley, P. M. (1998) The role of E6AP in the regulation of p53 protein levels in human papillomavirus (HPV)-positive and HPV-negative cells. *J. Biol. Chem.* **273,** 6439–6445
36. Lawson, J. S., Glenn, W. K., Heng, B., Ye, Y., Tran, B., Lutze-Mann, L., and Whitaker, N. J. (2009) Koilocytes indicate a role for human papilloma virus in breast cancer. *Br. J. Cancer* **101,** 1351–1356
37. Muench, P., Probst, S., Schuetz, J., Leiprecht, N., Busch, M., Wesselborg, S., Stubenrauch, F., and Iftner, T. (2010) Cutaneous papillomavirus E6 proteins must interact with p300 and block p53-mediated apoptosis for cellular immortalization and tumorigenesis. *Cancer Res.* **70,** 6913–6924
38. Munakata, T., Liang, Y., Kim, S., McGivern, D. R., Huibregtse, J., Nomoto, A., and Lemon, S. M. (2007) Hepatitis C virus induces E6AP-dependent degradation of the retinoblastoma protein. *PLoS Pathog.* **3,** 1335–1347
39. Shirakura, M., Murakami, K., Ichimura, T., Suzuki, R., Shimoji, T., Fukuda, K., Abe, K., Sato, S., Fukasawa, M., Yamakawa, Y., Nishijima, M., Moriishi, K., Matsuura, Y., Wakita, T., Suzuki, T., Howley, P. M., Miyamura, T., and Shoji, I. (2007) E6AP ubiquitin ligase mediates ubiquitylation and degradation of hepatitis C virus core protein. *J. Virol.* **81,** 1174–1185
40. Chen, J. J., Hong, Y., Rustamzadeh, E., Baleja, J. D., and Androphy, E. J. (1998) Identification of an α helical motif sufficient for association with papillomavirus E6. *J. Biol. Chem.* **273,** 13537–13544
41. Elston, R. C., Napthine, S., and Doorbar, J. (1998) The identification of a conserved binding motif within human papillomavirus type 16 E6 binding peptides, E6AP and E6BP. *J. Gen. Virol.* **79,** 371–374
42. Be, X., Hong, Y., Wei, J., Androphy, E. J., Chen, J. J., and Baleja, J. D. (2001) Solution structure determination and mutational analysis of the papillomavirus E6 interacting peptide of E6AP. *Biochemistry* **40,** 1293–1299
43. Liu, Y., Cherry, J. J., Dineen, J. V., Androphy, E. J., and Baleja, J. D. (2009) Determinants of stability for the E6 protein of papillomavirus type 16. *J. Mol. Biol.* **386,** 1123–1137
44. Zanier, K., Charbonnier, S., Baltzinger, M., Nominé, Y., Altschuh, D., and Travé, G. (2005) Kinetic analysis of the interactions of human papillomavirus E6 oncoproteins with the ubiquitin ligase E6AP using surface plasmon resonance. *J. Mol. Biol.* **349,** 401–412
45. Zanier, K., Ruhlmann, C., Melin, F., Masson, M., Ould M'hamed Ould Sidi, A., Bernard, X., Fischer, B., Brino, L., Ristriani, T., Rybin, V., Baltzinger, M., Vande Pol, S., Hellwig, P., Schultz, P., and Travé, G. (2010) E6 proteins from diverse papillomaviruses self-associate both *in vitro* and *in vivo*. *J. Mol. Biol.* **396,** 90–104
46. Zanier, K., Charbonnier, S., Sidi, A. O., McEwen, A. G., Ferrario, M. G., Poussin-Courmontagne, P., Cura, V., Brimer, N., Babah, K. O., Ansari, T., Muller, I., Stote, R. H., Cavarelli, J., Vande Pol, S., and Travé, G. (2013) Structural basis for hijacking of cellular LxxLL motifs by papillomavirus E6 oncoproteins. *Science* **339,** 694–698
47. Nominé, Y., Charbonnier, S., Ristriani, T., Stier, G., Masson, M., Cavusoglu, N., Van Dorsselaer, A., Weiss, E., Kieffer, B., and Travé, G. (2003) Domain substructure of HPV E6 oncoprotein. Biophysical characterization of the E6 C-terminal DNA-binding domain. *Biochemistry* **42,** 4909–4917
48. Kao, W. H., Beaudenon, S. L., Talis, A. L., Huibregtse, J. M., and Howley,

P. M. (2000) Human papillomavirus type 16 E6 induces self-ubiquitination of the E6AP ubiquitin-protein ligase. *J. Virol.* **74,** 6408–6417
49. Huang, L., Kinnucan, E., Wang, G., Beaudenon, S., Howley, P. M., Huibregtse, J. M., and Pavletich, N. P. (1999) Structure of an E6AP-UbcH7 complex. Insights into ubiquitination by the E2-E3 enzyme cascade. *Science* **286,** 1321–1326
50. Scheffner, M., Huibregtse, J. M., and Howley, P. M. (1994) Identification of a human ubiquitin-conjugating enzyme that mediates the E6-AP-dependent ubiquitination of p53. *Proc. Natl. Acad. Sci. U.S.A.* **91,** 8797–8801
51. Ronchi, V. P., Klein, J. M., and Haas, A. L. (2013) E6AP/UBE3A ubiquitin ligase harbors two E2∼ubiquitin binding sites. *J. Biol. Chem.* **288,** 10349–10360
52. Heer, A., Alonso, L. G., and de Prat-Gay, G. (2011) E6*, the 50 amino acid product of the most abundant spliced transcript of the e6 oncoprotein in high-risk human papillomavirus, is a promiscuous folder and binder. *Biochemistry* **50,** 1376–1383
53. Baboshina, O. V., and Haas, A. L. (1996) Novel multiubiquitin chain linkages catalyzed by the conjugating enzymes $E2_{epf}$ and Rad6 are recognized by the 26S proteasome subunit 5. *J. Biol. Chem.* **271,** 2823–2831
54. Haas, A. L. (2005) Purification of E1 and E1-like enzymes. *Methods Mol. Biol.* **301,** 23–35
55. Haas, A. L., and Rose, I. A. (1982) The mechanism of ubiquitin activating enzyme. A kinetic and equilibrium analysis. *J. Biol. Chem.* **257,** 10329–10337
56. Haas, A. L., and Bright, P. M. (1988) The resolution and characterization of putative ubiquitin carrier protein isozymes from rabbit reticulocytes. *J. Biol. Chem.* **263,** 13258–13267
57. Tokgöz, Z., Siepmann, T. J., Streich, F., Jr., Kumar, B., Klein, J. M., and Haas, A. L. (2012) E1-E2 interactions in ubiquitin and Nedd8 ligation pathways. *J. Biol. Chem.* **287,** 311–321
58. Ronchi, V. P., and Haas, A. L. (2012) Measuring rates of ubiquitin chain formation as a functional readout of ligase activity. *Methods Mol. Biol.* **832,** 197–218
59. Siepmann, T. J., Bohnsack, R. N., Tokgöz, Z., Baboshina, O. V., and Haas, A. L. (2003) Protein interactions within the N-end rule ubiquitin ligation pathway. *J. Biol. Chem.* **278,** 9448–9457
60. van Woerden, G. M., Harris, K. D., Hojjati, M. R., Gustin, R. M., Qiu, S., de Avila Freire, R., Jiang, Y. H., Elgersma, Y., and Weeber, E. J. (2007) Rescue of neurological deficits in a mouse model for Angelman syndrome by reduction of αCaMKII inhibitory phosphorylation. *Nat. Neurosci.* **10,** 280–282
61. Baboshina, O. V., Crinelli, R., Siepmann, T. J., and Haas, A. L. (2001) N-end rule specificity within the ubiquitin/proteasome pathway is not an affinity effect. *J. Biol. Chem.* **276,** 39428–39437
62. Davies, S. W., Turmaine, M., Cozens, B. A., DiFiglia, M., Sharp, A. H., Ross, C. A., Scherzinger, E., Wanker, E. E., Mangiarini, L., and Bates, G. P. (1997) Formation of neuronal intranuclear inclusions underlies the neurological dysfunction in mice transgenic for the HD mutation. *Cell* **90,** 537–548
63. Krissinel, E., and Henrick, K. (2007) Inference of macromolecular assemblies from crystalline state. *J. Mol. Biol.* **372,** 774–797
64. Maru, Y., Afar, D. E., Witte, O. N., and Shibuya, M. (1996) The dimerization property of glutathione *S*-transferase partially reactivates Bcr-Abl lacking the oligomerization domain. *J. Biol. Chem.* **271,** 15353–15357
65. Vargo, M. A., Nguyen, L., and Colman, R. F. (2004) Subunit interface residues of glutathione *S*-transferase A1–1 that are important in the monomer-dimer equilibrium. *Biochemistry* **43,** 3327–3335
66. Huang, Y. C., Misquitta, S., Blond, S. Y., Adams, E., and Colman, R. F. (2008) Catalytically active monomer of glutathione *S*-transferase π and key residues involved in the electrostatic interaction between subunits. *J. Biol. Chem.* **283,** 32880–32888
67. Levy, E. D., and Teichmann, S. (2013) Structural, evolutionary, and assembly principles of protein oligomerization. *Prog. Mol. Biol. Transl. Sci.* **117,** 25–51
68. Perica, T., Chothia, C., and Teichmann, S. A. (2012) Evolution of oligomeric state through geometric coupling of protein interfaces. *Proc. Natl. Acad. Sci. U.S.A.* **109,** 8127–8132
69. Verdecia, M. A., Joazeiro, C. A., Wells, N. J., Ferrer, J. L., Bowman, M. E., Hunter, T., and Noel, J. P. (2003) Conformational flexibility underlies ubiquitin ligation mediated by the WWP1 HECT domain E3 ligase. *Mol. Cell* **11,** 249–259
70. Ogunjimi, A. A., Wiesner, S., Briant, D. J., Varelas, X., Sicheri, F., Forman-Kay, J., and Wrana, J. L. (2010) The ubiquitin binding region of the Smurf HECT domain facilitates polyubiquitylation and binding of ubiquitylated substrates. *J. Biol. Chem.* **285,** 6308–6315
71. Pandya, R. K., Partridge, J. R., Love, K. R., Schwartz, T. U., and Ploegh, H. L. (2010) A structural element within the HUWE1 HECT domain modulates self-ubiquitination and substrate ubiquitination activities. *J. Biol. Chem.* **285,** 5664–5673
72. Maspero, E., Mari, S., Valentini, E., Musacchio, A., Fish, A., Pasqualato, S., and Polo, S. (2011) Structure of the HECT:ubiquitin complex and its role in ubiquitin chain elongation. *EMBO Rep.* **12,** 342–349
73. Kamadurai, H. B., Souphron, J., Scott, D. C., Duda, D. M., Miller, D. J., Stringer, D., Piper, R. C., and Schulman, B. A. (2009) Insights into ubiquitin transfer cascades from a structure of a UbcH5B approximately ubiquitin-HECT(NEDD4L) complex. *Mol. Cell* **36,** 1095–1102
74. Ogunjimi, A. A., Briant, D. J., Pece-Barbara, N., Le Roy, C., Di Guglielmo, G. M., Kavsak, P., Rasmussen, R. K., Seet, B. T., Sicheri, F., and Wrana, J. L. (2005) Regulation of Smurf2 ubiquitin ligase activity by anchoring the E2 to the HECT domain. *Mol. Cell* **19,** 297–308
75. Fang, P., Lev-Lehman, E., Tsai, T. F., Matsuura, T., Benton, C. S., Sutcliffe, J. S., Christian, S. L., Kubota, T., Halley, D. J., Meijers-Heijboer, H., Langlois, S., Graham, J. M., Jr., Beuten, J., Willems, P. J., Ledbetter, D. H., and Beaudet, A. L. (1999) The spectrum of mutations in UBE3A causing Angelman syndrome. *Hum. Mol. Genet.* **8,** 129–135
76. Chan, A. L., Grossman, T., Zuckerman, V., Campigli Di Giammartino, D., Moshel, O., Scheffner, M., Monahan, B., Pilling, P., Jiang, Y. H., Haupt, S., Schueler-Furman, O., and Haupt, Y. (2013) C-Abl phosphorylates E6AP and regulates its E3 ubiquitin ligase activity. *Biochemistry* **52,** 3119–3129
77. Scheffner, M., Werness, B. A., Huibregtse, J. M., Levine, A. J., and Howley, P. M. (1990) The E6 oncoprotein encoded by human papillomavirus types 16 and 18 promotes the degradation of p53. *Cell* **63,** 1129–1136
78. Huibregtse, J. M., Scheffner, M., and Howley, P. M. (1993) Localization of the E6-AP regions that direct human papillomavirus E6 binding, association with p53, and ubiquitination of associated proteins. *Mol. Cell Biol.* **13,** 4918–4927
79. Lagrange, M., Charbonnier, S., Orfanoudakis, G., Robinson, P., Zanier, K., Masson, M., Lutz, Y., Trave, G., Weiss, E., and Deryckere, F. (2005) Binding of human papillomavirus 16 E6 to p53 and E6AP is impaired by monoclonal antibodies directed against the second zinc-binding domain of E6. *J. Gen. Virol.* **86,** 1001–1007
80. Medcalf, E. A., and Milner, J. (1993) Targeting and degradation of p53 by E6 of human papillomavirus type 16 is preferential for the 1620+ p53 conformation. *Oncogene* **8,** 2847–2851
81. Thomas, M., Tomaić, V., Pim, D., Myers, M. P., Tommasino, M., and Banks, L. (2013) Interactions between E6AP and E6 proteins from α and β HPV types. *Virology* **435,** 357–362
82. Dai, B., Pieper, R. O., Li, D., Wei, P., Liu, M., Woo, S. Y., Aldape, K. D., Sawaya, R., Xie, K., and Huang, S. (2010) FoxM1B regulates NEDD4-1 expression, leading to cellular transformation and full malignant phenotype in immortalized human astrocytes. *Cancer Res.* **70,** 2951–2961
83. Marianayagam, N. J., Sunde, M., and Matthews, J. M. (2004) The power of two. Protein dimerization in biology. *Trends Biochem. Sci.* **29,** 618–625
84. Spitkovsky, D., Aengeneyndt, F., Braspenning, J., and von Knebel Doeberitz, M. (1996) p53-independent growth regulation of cervical cancer cells by the papillomavirus E6 oncogene. *Oncogene* **13,** 1027–1035
85. Streich, F. C., Jr., Ronchi, V. P., Connick, J. P., and Haas, A. L. (2013) TRIM ligases catalyze polyubiquitin chain formation through a cooperative allosteric mechanism. *J. Biol. Chem.* **288,** 8209–8221
86. Kiyono, T., Foster, S. A., Koop, J. I., McDougall, J. K., Galloway, D. A., and Klingelhutz, A. J. (1998) Both Rb/p16INK4a inactivation and telomerase activity are required to immortalize human epithelial cells. *Nature* **396,** 84–88
87. Kentsis, A., Gordon, R. E., and Borden, K. L. (2002) Control of biochemical

reactions through supramolecular RING domain self-assembly. *Proc. Natl. Acad. Sci. U.S.A.* **99,** 15404–15409
88. Sun, L., Deng, L., Ea, C. K., Xia, Z. P., and Chen, Z. J. (2004) The TRAF6 ubiquitin ligase and TAK1 kinase mediate IKK activation by BCL10 and MALT1 in T lymphocytes. *Mol. Cell* **14,** 289–301
89. Wang, X., Herr, R. A., Chua, W. J., Lybarger, L., Wiertz, E. J., and Hansen, T. H. (2007) Ubiquitination of serine, threonine, or lysine residues on the cytoplasmic tail can induce ERAD of MHC-I by viral E3 ligase mK3. *J. Cell Biol.* **177,** 613–624
90. Page, M. I., and Jencks, W. P. (1971) Entropic contributions to rate accelerations in enzymic and intramolecular reactions and the chelate effect. *Proc. Natl. Acad. Sci. U.S.A.* **68,** 1678–1683